Waste Management 161 (2023) 116–141

Contents lists available at ScienceDirect

Waste Management

journal homepage: www.elsevier.com/locate/wasman

On the use of plastic precursors for preparation of activated carbons and their evaluation in CO_2 capture for biogas upgrading: a review

S. Pérez-Huertas [a], M. Calero [a,*], A. Ligero [a], A. Pérez [a], K. Terpiłowski [b], M.A. Martín-Lara [a,*]

[a] Department of Chemical Engineering, University of Granada, 18071 Granada, Spain
[b] Department of Interfacial Phenomena, Maria Curie Skłodowska University, M. Curie Skłodowska Sq. 3, 20-031 Lublin, Poland

ARTICLE INFO

Keywords:
Activated carbons
Biogas upgrading
Char
CO_2 capture
Plastic waste
Pyrolysis

ABSTRACT

In circular economy, useful plastic materials are kept in circulation as opposed to being landfilled, incinerated, or leaked into the natural environment. Pyrolysis is a chemical recycling technique useful for unrecyclable plastic wastes that produce gas, liquid (oil), and solid (char) products. Although the pyrolysis technique has been extensively studied and there are several installations applying it on the industrial scale, no commercial applications for the solid product have been found yet. In this scenario, the use of plastic-based char for the biogas upgrading may be a sustainable way to transform the solid product of pyrolysis into a particularly beneficial material. This paper reviews the preparation and main parameters of the processes affecting the final textural properties of the plastic-based activated carbons. Moreover, the application of those materials for the CO_2 capture in the processes of biogas upgrading is largely discussed.

1. Introduction

Waste generation and management is becoming a growing global concern (Singh et al., 2014). In particular, the problem of handling plastic residues has attracted considerable attention during the last years (Bishop et al., 2020). These account for 85 % of the wastes getting into the oceans. By 2040 the amount of this material getting into the sea will have almost trebled, with an annual amount of 23–37 million tons (UNEP, 2021b). According to the comprehensive reports of the United Nations Environment Program (UNEP, 2021a), a drastic reduction of unnecessary, avoidable, and problematic plastic is crucial for handling the global pollution crisis. Plastic pollution is a growing threat in all ecosystems, with terrible consequences for the economy, biodiversity, and climate (Zheng and Suh, 2019). Human beings' health is also vulnerable to pollution caused by plastic (Almroth and Eggert, 2019). Plastics are found in seafood, drinks and even common salt, which results in the plastic contamination of the human food chain. Moreover, it also penetrates the skin and can be inhaled when suspended in the air. This might cause hormonal changes, developmental disorders, reproductive abnormalities, and even cancer (UNEP, 2021a). Furthermore, plastic contributes to the greenhouse gas (GHG) emissions from the beginning to the end of its life cycle (Ford et al., 2022). The contribution of plastic to climate change starts from the phase of raw materials extraction and is followed by plastic production, transport, use and disposal, as well as mismanaged waste and degradation. Additionally, plastic pollution also greatly affects the world economy. In 2028, the costs of plastic pollution in tourism, fishing, aquaculture, and other activities such as clean-ups were estimated to be US $ 6–19 billion. Moreover, by 2040 there could be an annual financial risk of US $ 100 billion for companies if governments require them to cover the waste management costs at the expected volumes (UNEP, 2021a).

On the other hand, most plastic materials are manufactured from fossil fuels that are non-renewable, finite resources. Interestingly, the increase in fuel and energy prices has resulted in a greater pressure on national economies. Thus, the scientific community must search for renewable substitutes to ensure cleaner and more environmentally friendly fuels (Ahmed et al., 2021). That is why the use of renewable energies is continuously growing due to their minor environmental impact on the decarbonized energy market (Khan et al., 2021). In this context, the chemical recycling of plastics can play a crucial role in the transition towards a circular economy and closed-loop recycling of plastic materials. Fig. 1 summarizes the main physical and chemical recycling methods used for plastic waste recycling. In particular, chemical recycling by pyrolysis enables the cracking of plastic wastes

* Corresponding authors.
E-mail addresses: shuertas@ugr.es (S. Pérez-Huertas), mcaleroh@ugr.es (M. Calero), aligero@correo.ugr.es (A. Ligero), aperezm@ugr.es (A. Pérez), terpil@umcs.pl (K. Terpiłowski), marianml@ugr.es (M.A. Martín-Lara).

https://doi.org/10.1016/j.wasman.2023.02.022
Received 5 August 2022; Received in revised form 17 February 2023; Accepted 20 February 2023

using thermal energy, which results in the production of solid (char), liquid (oil), and gas products.

In the past decades much attention was paid to oil and gas products. The produced liquid fraction can be refined into chemicals or fuels (Qureshi et al., 2020; Scott et al., 1990). However, studies on char applications, especially for the char derived from pyrolysis of plastic wastes, are more limited. Nevertheless, in recent years some researchers have investigated their use as adsorbent materials or precursors to produce activated carbons (Jamradloedluk and Lertsatitthanakorn, 2014; Martín-Lara et al., 2021).

Biogas is one of the most promising candidates in the renewable energies market. However, the raw gas contains a significant amount of CO_2 and other gases that limit its application. Currently, the removal of CO_2 from biogas is performed industrially by many commercial biogas upgrading technologies, such as pressure swing adsorption, chemical scrubbing, water scrubbing, organic solvent scrubbing, membrane separation or cryogenic separation (Golmakani et al., 2022). However, the use of these technologies involves large capital and operating costs, high energy consumption, corrosion potential and a significant loss of methane, leading to a lack of economic viability compared with natural gas from fossil fuel sources. Recently, the adsorptive CO_2 technology via solid porous adsorbents has become an attractive and promising technique for separating CO_2 from biogas because of its low energy demand and small capital investment compared to the conventional biogas upgrading methods. The adsorption efficiency depends on several factors such as the pore size of the adsorbent material, the partial pressure of the adsorbate, the system temperature and interaction forces between the adsorbate and the adsorbent material (Gunawardene et al., 2022). Different types of adsorbing materials are available for the separation of CO_2 from CH_4 in biogas. The adsorbents commonly used for the biogas upgrading process are zeolite (Gholipour and Mofarahi, 2016; Moura et al., 2016) and carbon-based adsorbents (Álvarez-Gutiérrez et al., 2018; Balsamo et al., 2013). Furthermore, innovative materials such as magnesium-based metal organic framework (MOF) silicalite (Li et al., 2011; Xian et al., 2015), silicoaluminophosphate sorbents (SAPOs) or polyethyleneimine-impregnated resins (Johnson et al., 2021) are also being considered for biogas upgrading. A careful analysis of the literature about biogas upgrading by adsorption on carbonaceous materials shows the following: a very few studies were carried out by dedicated experimental runs in the binary mixture (CO_2-CH_4) with the typical biogas composition of 40 % CO_2 / 60 % CH_4; most of the available data deal with the adsorption action of this mixture on a given adsorbent. Moreover, research on carbon-based adsorbents has been chiefly focused on biomass-derived carbons for that purpose.

To our knowledge, no studies have been reported on biogas upgrading by adsorption on carbonaceous materials obtained from the pyrolysis and further activation of plastic wastes. Although the plastic-based activated carbons showed interesting results as CO_2 adsorbents, they are largely untested in the upgrading of biogas and deserve further research. Therefore, there is a need to explore the associated benefits of using CO_2 adsorbents derived from plastic precursors for biogas upgrading. In this line, this research presents a comprehensive study that looks into the published data about the activated carbons derived from plastic wastes and estimates their use as CO_2 adsorbents for possible application in biogas upgrading. Hence, this review firstly provides insights into and guidelines for the preparation processes for matching the CO_2 adsorbent requirements; and secondly, it explores the potential of those materials for an alternative application and suggests further research directions.

The review is organized as follows: (a) A summary of plastic-based char production and its physicochemical characteristics is provided; (b) this is followed by a description and discussion of the most frequently used strategies for preparing activated carbons with tailored pore characteristics and their formation mechanisms; (c) an estimation of the potential of these materials for the CO_2 capture is presented; (d) biogas upgrading by residue-based activated carbons is discussed; (e) an overview of future avenues for research in the use of plastic-based activated carbons for biogas upgrading applications is given.

2. Production and activation of plastic-based char

2.1. Production and properties of plastic-based char

Pyrolysis is the main technique used for char production. It is a thermochemical process that degrades long-chain polymer macromolecules into simpler ones (mostly aliphatic and aromatic hydrocarbons) under a non-reactive atmosphere (Chen et al., 2020). High molecular weight organic polymers are uniformly heated to a specific temperature range and turned into high-quality oils, chars and gases without burning plastic wastes. Several mechanisms can take place during the pyrolysis of plastic wastes: chain scission, depolymerisation, cross-linking and chain stripping (Syamsiro et al., 2014). Char production by this recycling technique is a promising method, since the process conditions such as the temperature, heating rate and residence time can be manipulated to tailor the resulting product based on preferences (Wang et al., 2019; Zhang et al., 2020). According to these pyrolytic conditions, different types of processes are mainly classified into slow, fast and flash pyrolysis (Jahirul et al., 2012). Slow pyrolysis is typically used when the solid fraction (char) is the desired product; it is conducted at moderate temperatures (400–500 °C) during long residence times (5–30 min) and at slow heating rates (<10 °C/s). Fast pyrolysis is a rapid thermal decomposition mainly used to obtain the liquid product (oil); it is conducted at moderate to high temperatures (400–650 °C) during short residence times (0.5–10 s) and at high heating rates (10–200 °C/s). Flash pyrolysis is an extremely rapid thermal decomposition conducted at high temperatures (700–1000 °C) during very short residence times (<0.5 s) and at very high heating rates (>1000 °C/s); its major end-products are gases and bio-oil (Balat et al., 2009).

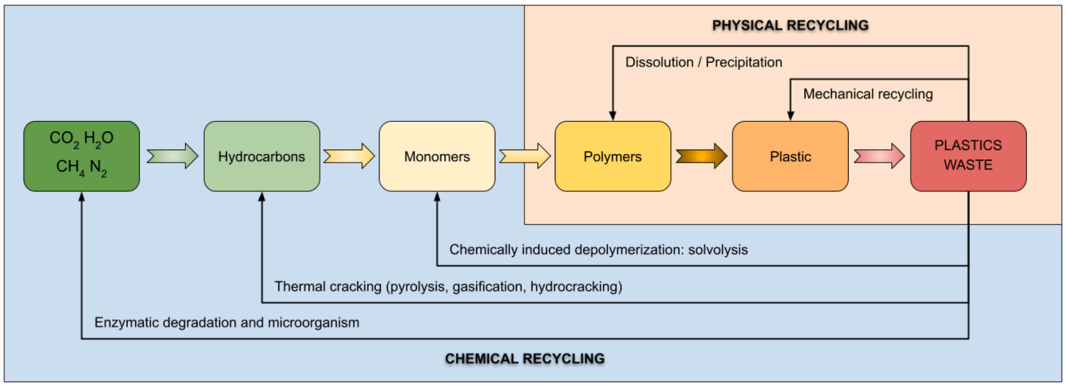

Fig. 1. Main physical and chemical recycling technologies for plastic waste recycling.

Different chemical reactors are currently used for the pyrolysis of plastic wastes. Several literature review manuscripts show the influence of those reactors on the product composition and distribution (Al-Salem et al., 2017; López et al., 2017; Solis and Silveira, 2020); the most frequently used include (a) laboratory-scale fixed-bed (Miandad et al., 2016), (b) fluidized-bed (Jung et al., 2010), (c) spouted-bed (Elordi et al., 2011), (d) horizontal tubular (Quesada et al., 2019), (e) screw kilns (Serrano et al., 2001), (f) microwave (Rosi et al., 2018) and (f) plasma reactors (Guddeti et al., 2000).

The laboratory scale fixed-bed reactors usually have a low capacity for the samples, generally not>500 g per batch. The volatiles usually pass through a condenser where the condensates are collected. The char residue remains in the reactor and can be removed after cooling. The reactor can be arranged horizontally or vertically, and heating is done

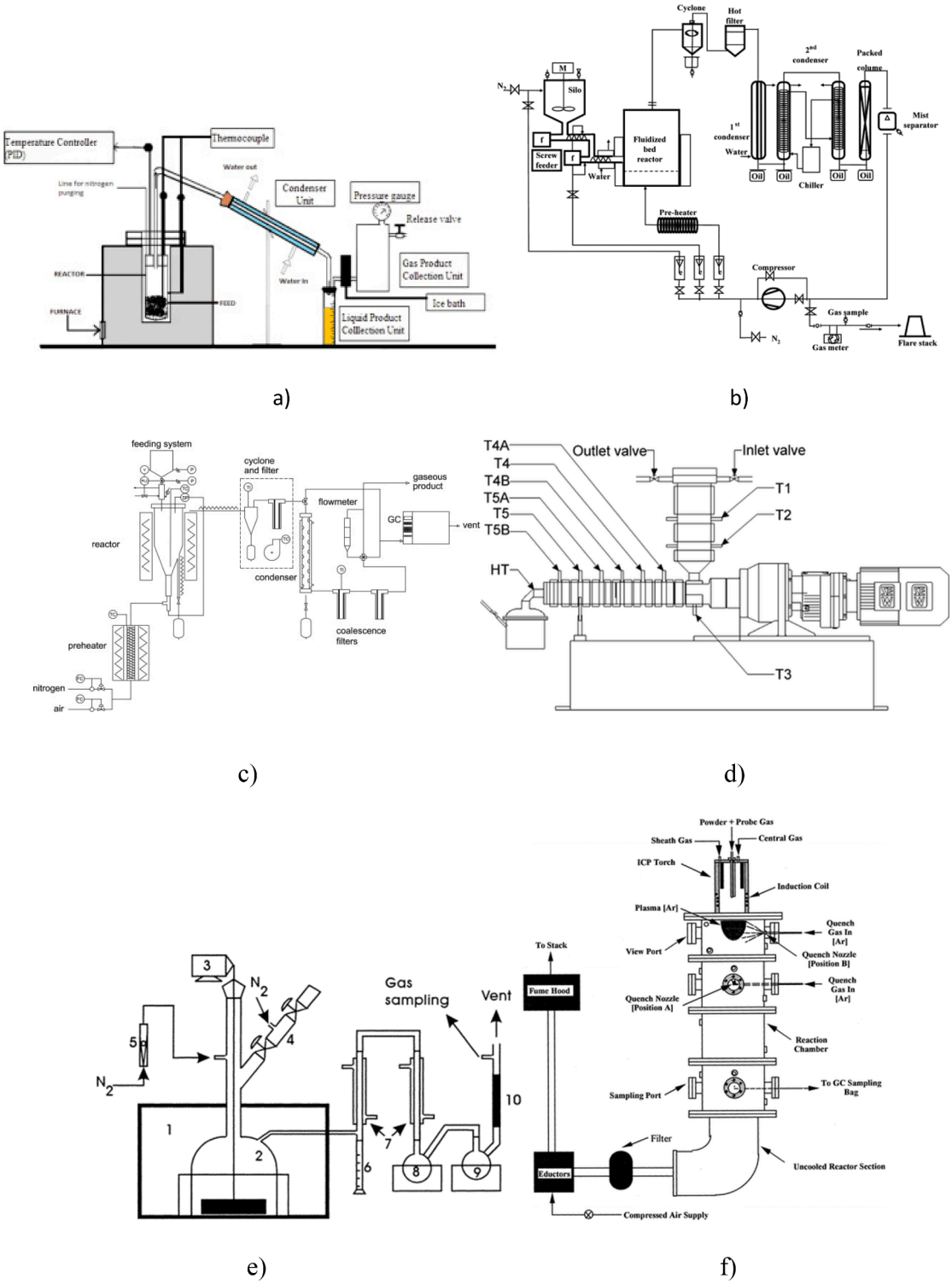

Fig. 2. Different pyrolysis reactors used currently for the pyrolysis of plastic waste: a) Laboratory scale fixed-bed (Singh et al., 2019a); b) Fluidized-bed (Kang et al., 2008); c) Spouted-bed (López et al., 2010); d) Screw kilns (Wallis et al., 2008); e) Microwave-assisted (Ludlow-Palafox and Chase, 2001); f) Induction-coupled plasma (Guddeti et al. 2000).

electrically, reaching temperatures of up to 900 °C. A scheme of this type of reactor is given in Fig. 2a (Singh et al., 2019a). These reactors are simple but have some important disadvantages such as long residence times and low heating rates, which results in a low heat transfer coefficient and a non-uniform temperature in the samples. Moreover, they also present difficulties in removing the char. The fluidized-bed reactors consist of four parts: (1) a feeding system, generally by means of a screw feeder; (2) the fluidized-bed reactor; (3) a cooling system by means of condensers for oil collection; and (4) a solid particle separation system, frequently composed of a cyclone and either one or several hot filters. These reactors, which have a vertical layout, are heated electrically, reaching temperatures of up to 900 °C. The feeding speed is variable, depending on the installation size and can vary from values of 100–200 g h^{-1} to several kg h^{-1}. Fig. 2b shows the diagram of the fluidized-bed plant (Kang et al., 2008). Although they have a simple design, are easy to operate and suitable for large scale, small particle sizes are required. It is worth noting that this type of reactor is the best for catalytic pyrolysis of plastic wastes. The catalyst might be regenerated several times without discharging, which is worth considering especially when the catalyst is expensive (Sharuddin et al., 2016).

The spouted-bed reactors have a conical geometry with a cylindrical upper section. The dimensions are variable depending on the installation size and are designed to guarantee the stability of the bed in different operating regimes. The other elements accompanying the reactor are similar to the other installations, mainly a condensation system for oil collection and cyclones and/or filters to retain particles. The heating system is usually powered and the operating temperatures are similar to those of the other types of reactors. Before entering the reactor, the nitrogen flow is preheated until it reaches the reaction temperature. Plastic precursors with larger particles and different densities can be used in this reactor, avoiding the need for their separation. However, this has some disadvantages such as the collection of the solid and liquid products. Fig. 2c presents the diagram of the pyrolysis installation with the spouted-bed reactor (López et al., 2010).

In the screw kilns reactors, pyrolysis is conducted in a screw extruder with different heating zones (Fig. 2d) (Wallis et al., 2008). The plastic material is melted in the feed hopper, which is heated and nitrogen-fed to keep the medium inert. The reaction zone is made up of a screw whose speed can be adjusted in different ranges by means of an electric motor to achieve the desired operating conditions. The different heating zones are controlled by thermocouples. At the exit of the extruder there is a condenser to collect the condensable liquid fraction. This type of reactor is one of the most widely used for the pyrolysis of plastic wastes because they are easy to operate and provide good temperature control. The stirrer enhances the heat transfer and its distribution and recovers the char remaining from the walls, which would otherwise behave as heat insulators (Butler and Devlin, 2011). Less favourably, these reactors require frequent maintenance.

Microwave-assisted pyrolysis has several advantages compared to the conventional heating modes, such as fast and homogeneous heating of the raw material and faster response to switching on and off. Generally, the reactor consists of a microwave oven inside which there is a container that is irradiated with microwaves and kept under agitation. The reactor temperature, which can reach up to 1000 °C, is controlled by thermocouples. The pyrolysis gases leave the reactor and pass through the system of condensers using a system that is similar to that mentioned above. Fig. 2e shows Ludlow-Palafox and Chase's (2001) experimental microwave-assisted pyrolysis equipment applied for plastic waste pyrolysis. The effectiveness of the microwave heating relies upon the dielectric properties of the precursor. For instance, given that plastics have a low dielectric constant, mixing them with carbon can enhance the energy absorbed to be transformed into heat in a shorter time (Lam and Chase, 2012). The most important disadvantages of this configuration are the high operating costs and high electrical power consumption.

Recently, plasma pyrolysis has been considered an appropriate method for the treatment of mixed plastic wastes, integrating the conditions of conventional pyrolysis with the properties of plasma. The temperatures obtained are very high, and the process is extremely fast, which is an advantage over the conventional system. However, the operation cost poses a problem in its application on the industrial scale. Guddeti et al. (2000) describe in detail the operation of an induction-coupled plasma reactor for the depolymerization of polypropylene (Fig. 2f). In conclusion, there are a variety of reactor configurations for plastic pyrolysis and these vary primarily in their solids handling, mixing, and heat transfer mechanisms. Nevertheless, while the reactor design affects the yield of the obtained pyrolytic products, the main factors influencing the production of the char are those associated with the pyrolysis process. In any case, some other hybrid energy systems with renewable energy sources are needed to explore cost-effective and energy-efficient pyrolysis reactors to solve the main disadvantages of some promising pyrolysis reactors, such as microwave-assisted or plasma pyrolysis reactors.

Table 1 summarizes the pyrolytic conditions and the solid yield obtained from different plastic wastes. In experimental conditions, the char yield varied considerably. As a matter of fact, in some cases no char was obtained. For example, FakhrHoseini and Dastanian (2013) reported solid yields of 0.0 % and 8.98 % for pyrolyzed polypropylene and polyethylene terephthalate, respectively, working under the same operation conditions. Similar findings were reported by Williams and Slaney (2007) using polystyrene and high-density polyethylene as the precursors. The authors reported a solid yield of 27 % for the former and 0 % for the latter. Thus, the nature of the precursor influences the char production. The pyrolysis temperature and heating rate are the most determinant factors influencing the char yield. Higher pyrolysis temperatures result in increased devolatilization of volatile matter, which is released from the plastic waste during the pyrolysis, producing a smaller char yield for the fixed heating rate (Peng et al., 2000). Demirbas (2004) studied the char yields of municipal plastic wastes at different temperatures. The solid product yield decreased from 38 % to 5 % with the increase of the pyrolysis temperature from 337 to 437 °C. Moreover, no solid fraction was obtained at temperatures higher than 527 °C. Miskolczi et al. (2004) studied the char yields of HDPE waste at different temperatures and found that the solid yields decreased with the increasing process temperature; at 400 °C, the solid product yield was 93.5 %. However, as the temperature increased up to 450 °C, the solid yield decreased to 19.7 %. Additionally, the authors also studied the effect of different catalysts, HZSM-5 and clinoptilolite, in the yield products. It was found that the yields of both gas and liquid fractions were larger when using these catalysts. However, as far as the temperature is concerned, the solid fraction yield was smaller. Therefore, the main variables affecting the final plastic-based char yield are: (1) the nature of the precursor, (2) the pyrolysis operating conditions, and (3) the use of a proper catalyst. Furthermore, the pyrolysis conditions also affect the resulting carbon properties and the subsequent application. Since they affect the cracking reactions, the temperature and heating rate are the dominant parameters controlling the final textural characteristics of the char. Generally, fast pyrolysis produces carbons with larger pores than those obtained by slower pyrolysis; moreover, a higher carbon yield is obtained from the latter. Whilst low heating rates produce carbons with abundant micropores, higher heating rates induce the formation of macropores in the resulting material, due to a faster devolatilization process (Cetin et al., 2004). Another concern of producing char at a high heating rate is its tendency to quickly chemi-sorb large amounts of O_2 when exposed to the air, which would reduce its surface area and active sites (Nsakala et al., 1978). Therefore, low temperatures and low heating rates are the most appropriate pyrolytic conditions to produce CO_2 adsorbents derived form plastic wastes.

Proximate or elemental analyses are usually performed to determine the char composition (i.e., moisture, ash, volatiles, and fixed carbon); on the other hand, chemical species (i.e. carbon, hydrogen, oxygen, nitrogen, sulphur, or chlorine) are obtained through the elemental analyses

Table 1
Summary of studies on pyrolyzed plastic waste.

Type of Plastic	Pyrolysis T. °C	Reactor	Heating rate °C min^{-1}	Holding time h	Catalyst	Solid yield (wt%)	Reference
LDPE 31.25 % + HDPE 31.25 % + PP 7.29 % + PS 13.50 % + PVC 11.46 % + PET% 5.21	500	Fluidized-bed	NA	0.02	–	2.82	(Williams and Williams, 1997a)
	550		NA	0.02	–	5.87	(Williams and Williams, 1997a)
	600		NA	0.02	–	7.59	(Williams and Williams, 1997a)
HDPE	700	Fixed-bed	25	Until no more gas was produced	–	0	(Williams and Williams, 1997b)
LDPE	700		25	Until no more gas was produced	–	0	(Williams and Williams, 1997b)
PS	700		25	Until no more gas was produced	–	3.50	(Williams and Williams, 1997b)
PP	700		25	Until no more gas was produced	–	0.15	(Williams and Williams, 1997b)
PET	700		25	Until no more gas was produced	–	15.55	(Williams and Williams, 1997b)
PVC	700		25	Until no more gas was produced	–	13.78	(Williams and Williams, 1997b)
LDPE 31.25 % + HDPE 31.25 % + PP 7.29 % + PS 13.50 % + PVC 11.46 % + PET 5.21 %	700		25	Until no more gas was produced	–	2.87	(Williams and Williams, 1997b)
Tyre	400	Unstirred batch	NA	NA	–	50.10	(Mui et al., 2010)
	500		NA	NA	–	37.15	(Mui et al., 2010)
	600		NA	NA	–	35.43	(Mui et al., 2010)
	700		NA	NA	–	34.93	(Mui et al., 2010)
	800		NA	NA	–	33.71	(Mui et al., 2010)
	900		NA	NA	–	32.34	(Mui et al., 2010)
	500		5	1	–	38.45	(Mui et al., 2010)
	500		5	2	–	37.15	(Mui et al., 2010)
	500		5	3	–	37.05	(Mui et al., 2010)
	500		5	4	–	35.66	(Mui et al., 2010)
	500		1	2	–	38.7	(Mui et al., 2010)
	500		5	2	–	37.15	(Mui et al., 2010)
	500		10	2	–	37	(Mui et al., 2010)
	500		15	2	–	36.9	(Mui et al., 2010)
	500		20	2	–	36.8	(Mui et al., 2010)
Real sample: PE 35 %, PP 40 %, PS 19 %, PET 5 %, PVC 1 %	500	Unstirred semi-batch	20	0.5	–	5.3	(Adrados et al., 2012)
Simulated sample: PE 40 %, PP 35 %, PS 18 %, PET 4 %, PVC 3 %	500		20	0.5	–	0.8	(Adrados et al., 2012)
	500		20	0.5	Red mud	0.6	(Adrados et al., 2012)
PS + PE + PP	337	Fixed-bed	10 K/s	NA	–	≈ 38	(Demirbas, 2004)
	427		10 K/s	NA	–	≈ 5	(Demirbas, 2004)
	527		10 K/s	NA	–	0	(Demirbas, 2004)
	627		10 K/s	NA	–	0	(Demirbas, 2004)
PE 58.6 %, PP 26.9 %, PS 8.8 %, PET 5.6 %	500	Fixed-bed	10	Non-isothermal		10 ± 1.2	(Singh et al., 2019a)
	500		20	Non-isothermal		8.5 ± 1.1	(Singh et al., 2019a)
	500		20 °C/s	Isothermal		2 ± 1	(Singh et al., 2019a)
PE 58.6 %, PP 26.9 %, PS 8.7 %, PET 5.6 %	450		20	1	–	≈ 11.5	(Singh and Ruj, 2016)
	500		20	1	–	9.5	(Singh and Ruj, 2016)
	550		20	1	–	≈ 6.5	(Singh and Ruj, 2016)
	600		20	1	–	≈ 3.8	(Singh and Ruj, 2016)
HDPE	400	Unstirred batch	NA	1	–	93.5	(Miskolczi et al., 2004)
	400		NA	1	NCM	90.6	(Miskolczi et al., 2004)
	400		NA	1	FCC	78.9	(Miskolczi et al., 2004)
	400		NA	1	HZSM-5	73.7	(Miskolczi et al., 2004)
	420		NA	1	–	85.6	(Miskolczi et al., 2004)
	420		NA	1	NCM	66.0	(Miskolczi et al., 2004)
	420		NA	1	FCC	64.1	(Miskolczi et al., 2004)
	420		NA	1	HZSM-5	55.4	(Miskolczi et al., 2004)
	450		NA	1	–	19.7	(Miskolczi et al., 2004)
	450		NA	1	NCM	15.2	(Miskolczi et al., 2004)
	450		NA	1	FCC	11.2	(Miskolczi et al., 2004)
	450		NA	1	HZSM-5	3.9	(Miskolczi et al., 2004)
HDPE	430	Fixed-bed	3	NA	–	9.0	(Uddin et al., 1997)
LDPE	430		3	NA	–	7.5	(Uddin et al., 1997)
HDPE	430		3	NA	SA-2	11.0	(Uddin et al., 1997)
LDPE	430		3	NA	SA-2	9.0	(Uddin et al., 1997)
LDPE	500	Fixed-bed	6	NA	–	0.16	(FakhrHoseini and Dastanian, 2013)

(*continued on next page*)

Table 1 (*continued*)

Type of Plastic	Pyrolysis T. °C	Reactor	Heating rate °C min^{-1}	Holding time h	Catalyst	Solid yield (wt%)	Reference
	500		10	NA	–	0.09	(FakhrHoseini and Dastanian, 2013)
	500		14	NA	–	0.04	(FakhrHoseini and Dastanian, 2013)
PET	500		6	NA	–	8.98	(FakhrHoseini and Dastanian, 2013)
	500		10	NA	–	7.64	(FakhrHoseini and Dastanian, 2013)
	500		14	NA	–	5.74	(FakhrHoseini and Dastanian, 2013)
PP	500		6	NA	–	0.12	(FakhrHoseini and Dastanian, 2013)
	500		10	NA	–	0.07	(FakhrHoseini and Dastanian, 2013)
	500		14	NA	–	0.0	(FakhrHoseini and Dastanian, 2013)
LDPE	425	Pressurised batch	10	1	–	0.5	(Onwudili et al., 2009)
	450		10	1	–	1.75	(Onwudili et al., 2009)
	500		10	1	–	15.5	(Onwudili et al., 2009)
PS	350		10	1	–	1	(Onwudili et al., 2009)
	450		10	1	–	19.6	(Onwudili et al., 2009)
	500		10	1	–	30.4	(Onwudili et al., 2009)
LDPE 70 % PS 30 %	400		10	1	–	0	(Onwudili et al., 2009)
	425		10	1	–	1.2	(Onwudili et al., 2009)
	450		10	1	–	3.5	(Onwudili et al., 2009)
HDPE	500	Pressurised batch	5	1	–	0	(Williams and Slaney, 2007)
PP	500		5	1	–	0	(Williams and Slaney, 2007)
PS	500		5	1	–	27	(Williams and Slaney, 2007)
PET	500		5	1	–	53	(Williams and Slaney, 2007)
PE 40 %, PP 35 %, PS 18 %, PET 4 %, PVC 3 %	500	Unstirred semi-batch	20	0.5	–	0.8	(López et al., 2011a)
PE 40 %, PP 35 %, PS 18 %, PET 4 %, PVC 3 %	460		20	0.5	–	1.1	(López et al., 2011b)
	500		20	0.5	–	0.8	(López et al., 2011b)
	600		20	0.5	–	0.9	(López et al., 2011b)
	500		20	0 min	–	24.1	(López et al., 2011b)
	500		20	0.25	–	≈1	(López et al., 2011b)
	500		20	0.5	–	≈1	(López et al., 2011b)
	500		20	2	–	≈1	(López et al., 2011b)
PET	725	Fixed-bed	NA	NA	NA	22	(Parra et al., 2006)

(Saptoadi et al., 2016). Table 2 shows the elemental composition of the plastic-based char from a series of studies. Similarly to hydrocarbons, plastic char is characterized by a large carbon content, in most cases over 70 % or even up to 99 % (Parra et al., 2006). The pyrolysis temperature not only affects the char yield but also its composition. The higher the pyrolysis temperature, the higher the char carbon content. However, the O and H contents decrease, since their respective functional groups are released as volatile matter during the decomposition reactions (López et al., 2011b). These transformations induce the development of porosity in the resulting carbon material.

The results from the proximate analysis of the plastic-based chars are also given in Table 2. Their common characteristics include a small moisture and ash content with a larger content of volatile and fixed carbon. According to Saptoadi et al. (2016), the contents of the plastic-based char components are dependent on the nature of the precursor, the operating temperature, and the use of suitable catalysts. A low ash content is favourable for developing efficient CO_2 adsorbent materials. A large ash content may cover the pores, reducing the surface area and creating internal heat and mass transfer limitations (Gray et al., 2002).

2.2. Preparation of activated carbons

It is well known that the use of plastic wastes to produce gaseous pollutant adsorbents can solve two key environmental issues: the management of residues and the control of the CO_2 emissions level. That is why it is paramount to focus on the role played by activated carbon, which can be produced, among others, after char activation. Carbon materials can be activated by either physical or chemical processes. Fig. 3 summarizes the general procedure used for both activation methods. In the chemical activation, the precursor is first subjected to a pyrolysis process to remove the non-carbon elements, producing the char. Then, the char is mixed with a chemical agent (such as KOH, NaOH, K_2CO_3 or H_3PO_4), whose main role is to degrade the precursor (Kaur et al., 2019b). At that point, the mixture is subjected to a new thermal process in an inert environment. In some other cases, the chemical activation is a single-step process, where the carbonization and activation are performed simultaneously. In any case, once the thermal treatment is over, the solid product is washed with deionized water and/or acid, depending on the chemical agent used (Namane et al., 2005). The washing process aims at removing the chemical components in the remaining material (Singh et al., 2019b). Finally, the product is dried in an oven until its weight remains constant. The remaining material is an activated carbon in which the size and number of pores are increased significantly.

Physical activation can also be performed as a one-step or two-step process. In the two-step process, as in the chemical activation, the material is first pyrolyzed in an inert atmosphere, producing carbon with a porous structure that is not very refined. In the activation stage, a second

Table 2
Summary of chemical properties of the plastic-based chars.

Type of Plastic	Pyrolysis conditions	Reactor	Moisture	Volatile matter	Fixed carbon	Ash	C	H	N	Cl	O	Reference
HDPE	Fast pyrolysis 400–450 °C	Fixed-bed	2.41	51.40	46.03	0.16	42.65	3.06	0.43	–	1.80	(Jamradloedluk and Lertsatitthanakorn, 2014)
LDPE 31.25 % + HDPE 31.25 % + PP 7.29 % + PS 13.50 % + PVC 11.46 % + PET 5.21 %	500 °C – 15 s	Fluidised bed	–	–	–	96.92	1.73	0.07	0.05	–	–	(Williams and Williams, 1997a)
	600 °C – 15 s		–	–	–	77.86	2.35	0.08	0.02	–	–	(Williams and Williams, 1997a)
	700 °C – 15 s		–	–	–	53.81	34.53	0.51	0.77	–	–	(Williams and Williams, 1997a)
LDPE 31.25 % + HDPE 31.25 % + PP 7.29 % + PS 13.50 % + PVC 11.46 % + PET 5.21 %	700 °C until no more gas was produced	Fixed-bed	–	–	–	4.23	87.73	1.99	0.13	–	–	(Williams and Williams, 1997b)
PET	700 °C until no more gas was produced		–	–	–	5.86	84.93	2.48	0	–	–	(Williams and Williams, 1997b)
PVC	700 °C until no more gas was produced		–	–	–	2.91	90.15	2.55	0.15	–	–	(Williams and Williams, 1997b)
PE	450 °C		5.80	55.46	15.15	23.57	–	–	–	–	–	(Saptoadi et al., 2016)
PE 50 % + PP 40 % + PS 10 %	Natural Zeolite catalyst	NA	10.36	17.12	43.00	29.50	–	–	–	–	–	(Saptoadi et al., 2016)
PE	500 °C Natural Zeolite catalyst		9.28	24.68	24.97	41.05	–	–	–	–	–	(Saptoadi et al., 2016)
PE + Others (50:50)	450 °C		4.68	6.23	52.56	36.50	–	–	–	–	–	(Saptoadi et al., 2016)
PE + PS (50:50)	Natural Zeolite catalyst		4.39	63.67	9.89	22.03	–	–	–	–	–	(Saptoadi et al., 2016)
Real sample 35 % PE, 40 % PP, 19 % PS, 5 % PET, 1 % PVC	500 °C – 30 min	Unstirred semi-batch	2.3	–	–	61.4	29.3	1.2	1.1	4.7	–	(Adrados et al., 2012)
Simulated sample 40 % PE, 35 % PP, 18 % PS, 4 % PET, 3 % PVC			0.2	–	–	2.3	93.7	3.5	–	0.3	–	(Adrados et al., 2012)
	Red mud catalyst		0.9	–	–	80.8	13.9	0.7	–	3.7	–	(Adrados et al., 2012)
PET	700 °C – 2 h		–	–	–	–	81.22	2.27	–	–	11.71	(Kaur et al., 2019a)
	500–800 °C- 2 h + KOH act.	Fixed-bed	–	–	–	–	80.38	0.63	–	–	18.99	(Kaur et al., 2019a)
	500–800 °C- 2 h + KOH act.		–	–	–	–	65.10	0.57	–	–	34.33	(Kaur et al., 2019a)
PE 40 %, PP 35 %, PS 18 %, PET 4 %, PVC 3 %	460 °C- 30 min	Unstirred semi-batch	0.1	–	–	–	92.0	3.9	–	0.1	–	(López et al., 2011b)
	500 °C –30 min		0.2	–	–	–	93.7	3.5	–	0.3	–	(López et al., 2011b)
	600 °C – 30 min		0.1	–	–	–	91.7	2.3	–	0.3	–	(López et al., 2011b)
	500 °C –15 min		0.4	–	–	–	94.4	3.7	–	0.2	–	(López et al., 2011b)
	500 °C – 30 min		0.2	–	–	–	93.7	3.5	–	0.3	–	(López et al., 2011b)
	500 °C – 120 min		0.3	–	–	–	94.1	3.5	–	0.1	–	(López et al., 2011b)
PET	725 °C – 1 h		–	–	–	–	96.6	1.8	–	–	1.2	(Parra et al., 2006)
	+ CO_2 act. –1h	Fixed-bed	–	–	–	–	98.2	0.5	–	–	0.9	(Parra et al., 2006)
	+ CO_2 act. –12 %*		–	–	–	–	98.8	0.3	–	–	0.6	(Parra et al., 2006)
	+ CO_2 act. –35 %*		–	–	–	–	98.9	0.3	–	–	0.6	(Parra et al., 2006)
	+ CO_2 act. –58 %*		–	–	–	–	98.7	0.2	–	–	0.6	(Parra et al., 2006)
	+ CO_2 act. –76 %*		–	–	–	–	99.0	0.2	–	–	0.5	(Parra et al., 2006)

(continued on next page)

Table 2 (*continued*)

Type of Plastic	Pyrolysis conditions	Reactor	Moisture	Volatile matter	Fixed carbon	Ash	C	H	N	Cl	O	Reference
PET	700 °C –2h	Fixed-bed	–	–	–	–	≈82	≈2.5	–	–	11.71	(Kaur et al., 2019b)
	+ KOH act. (1:1)		–	–	–	–	80	<1	–	–	18.99	(Kaur et al., 2019b)
	+ KOH act. (2:1)		–	–	–	–	≈68	<1	–	–	≈31	(Kaur et al., 2019b)
	+ KOH act. (3:1)		–	–	–	–	65.1	<1	–	–	34.33	(Kaur et al., 2019b)
	+ KOH act. (4:1)		–	–	–	–	≈70	<1	–	–	≈30	(Kaur et al., 2019b)
PET	500 °C – 0.5 h KOH act.	Horizontal tubular	–	–	–	–	81.3	2.7	–	–	16.0	(Arenillas et al., 2005)
	+ Acridine		–	–	–	–	73.7	3.1	0.5	–	22.7	(Arenillas et al., 2005)
	+ Carbazole		–	–	–	–	75.2	2.8	4.2	–	17.8	(Arenillas et al., 2005)
	+ Urea		–	–	–	–	75.2	2.6	0.5	–	21.7	(Arenillas et al., 2005)

*Burn-off degree.

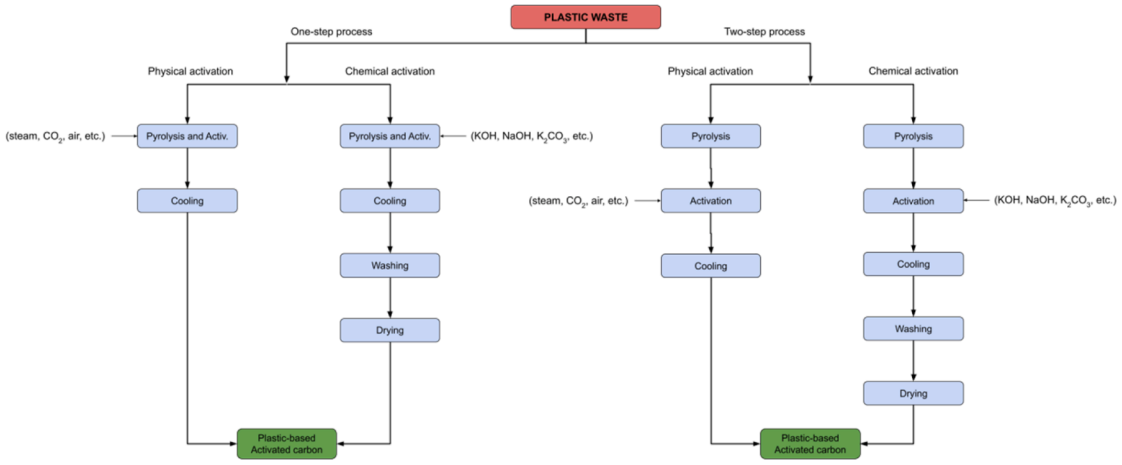

Fig. 3. Schematic diagram of activated carbon preparation from the plastic waste.

heating proceeds in the presence of such oxidizing agents as steam, carbon dioxide, air or their binary mixture (Rodríguez-Reinoso and Molina-Sabio, 1992). The gasification opens and develops the pores to the most convenient size and shapes, depending on the gas and the operating conditions (Choma et al., 2016).

Besides the method selected for the preparation of activated carbon, the choice of the precursor is also of great importance (Bhatnagar et al., 2013). The nature of the precursor contributes to the final porous texture of the carbon materials. The use of different precursors to produce porous carbon has been extensively researched. These studies can be classified into two groups: naturally occurring (cellulosic and lignocellulosic) and synthetic (polymers) precursors. The former is the most investigated low-cost precursor (Ioannidou and Zabaniotou, 2007). Interestingly, the use of polymer wastes as a precursor for the preparation of CO_2 adsorbents seems to provide a better control to achieve enhanced morphology, a tuneable pore system, functionality, and specific surface chemistry as compared to those obtained from biomass wastes (Zhang et al., 2015).

3. The effect of the activation method on the textural parameters of plastic-based activated carbons

3.1. Effects under chemical activation conditions

Obtaining a suitable pore structure is the main aim in the synthesis of any effective CO_2 adsorbent material. It should have a large surface area and abundant micropores of the appropriate size to match the CO_2 molecules. The porosity of the activated carbons is the main parameter that can be tailored by controlling the experimental variables involved in the chemical activation process, e.g., the activation temperature and time, chemical agent, impregnation ratio or flow rate.

3.1.1. Activation with KOH

Potassium hydroxide is the most frequently used agent for the activation of porous carbon obtained from plastic wastes. This chemical is a strong and corrosive base that melts without decomposition at 360 °C (Bailar and Trotaman-Dickenson, 1973). Moreover, at that temperature, it can react with most carbon materials. The following possible reactions between potassium hydroxide and pyrolyzed carbon occurring during the activation have been reported so far (Wang and Kaskel, 2012):

$2KOH \rightarrow K_2O + H_2O$ (Potassium hydroxide is dehydrated at ≈ 400 °C)(R.1)

$C + H_2O \rightarrow CO + H_2$ (Water-gas reaction)(R.2)

$CO + H_2O \rightarrow CO_2 + H_2$ (Water-gas shift reaction)(R.3)

$CO_2 + K_2O \rightarrow K_2CO_3$ (Potassium carbonate formed at ≈ 400–500 °C)(R.4)

$6KOH + 2C \rightarrow 2\,K + 3H_2 + 2K_2CO_3$ (Potassium hydroxide is consumed at ≈ 600 °C)(R.5)

$K_2CO_3 \rightarrow K_2O + CO_2$ (Potassium carbonate is decomposed at ≈ 700 °C)(R.6)

$CO_2 + C \rightarrow 2CO$(R.7)

$K_2CO_3 + 2C \rightarrow 2\,K + 3CO$ (Potassium oxide compounds are reduced at ≈ T > 700 °C)(R.8)

Table 3
Summary of the operating conditions during the activation of plastic material precursors with KOH and their textural properties.

Precursor	Pyrolysis T/°C – t/ h	Activation T/ °C – t/ h	N_2 Flow Rate mL min^{-1}	Agent/ Precursor ratio	S_{BET} m^2 g^{-1}	Pore Vol. cm^3 g^{-1}	Reference
Polyacrylonitrile PAN	800–2	800–2	60	2:1	1,513	0.65	(Singh et al., 2019c)
				3:1	1,884	1.34	
				4:1	1,694	0.96	
PAN	800–2	800–2	50	3:1	1,890	1.47	(Singh et al., 2019b)
Polyethylene terephthalate PET	600–1	700–1	200	2:1	1,812	0.75	(Yuan et al. 2020a)
		1,000–1			1,689	0.78	
Polyurethane Foam PU-F	400–1	700–2	60	2:1	1,360	0.59	(Ge et al., 2019)
PET	700–2	700–2	60	1:1	591	0.26	(Kaur et al., 2019b)
				3:1	1,690	0.83	
				4:1	1,280	0.66	
Polystyrene Foam PS-F	500–5	600–1	–	4:1	2,109	0.88	(De Paula et al., 2018)
		800–1			2,712	1.2	
PU-F	400–1	700–2	80	1:1	1,516	0.64	(Ge et al., 2016)
				2:1	1,430	0.59	
				4:1	1,420	0.58	
PU-F	700–1	Single-step	80	2:1	1,077	0.70	(Ge et al., 2016)
Kevlar	500 – 0.5	700–0.5	900	3:1	1,830	1.26	(Choma et al. 2014)
				4:1	2,660	1.54	
				5:1	2,450	1.41	
PAN	850–2	Single-Step	50	2:1	780	0.39	(Shen et al., 2011)
	500–2	850–1			2,231	1.16	
PET	1) 400–1 2) 800–1	Single-step	50	1:1	1,338	0.79	(Adibfar et al., 2014)
PAN pre-oxidized with $ZnCl_2$	800–1	Single-step	20	0.8:1	3,072	1.75	(Kamran et al., 2020)
PAN pre-oxidized with $ZnCl_2$	800–1	Single-step	20	0.8:1	1,167	0.59	(Feng et al., 2018)
				0.6:1	2,151	1.11	
PAN pre-oxidized with KNO_3	750–2	Single-step	–	3:1	3,751	2.48	(Li et al., 2019b)
PAN pre-oxidized with KNO_3	750–2	Single-step	–	1:1	2,568	1.15	(Li et al., 2019a)
				2:1	2,927	1.54	
				3:1	2,870	1.69	
PAN dissolved in NN-dimethylacetamide	220–1.5	900–3	1,500	3:1	2,366	0.83	(Hsiao et al., 2011)
	240–1.5				3,275	1.51	
	280–1.5				2,655	0.14	
PET	600–1	850–1.5	–	2:1	2,831	1.68	(Lian et al., 2011)
Polyvinyl chloride PVC	600–1	850–1.5	–	2:1	2,666	1.44	(Lian et al., 2011)
PS	700–2	770–1	–	2:1	1,566	1.05	(Wang et al., 2009)
				3:1	1,708	1.19	
				4:1	2,022	1.35	
PET	700–1	Single-step	100	1:1	454	–	(Almazán-Almazán et al., 2007)
				2:1	1,026		
				3:1	1,308		
PET	700–1	Single-step	100	1:1	454	–	(Almazán-Almazán et al., 2010)
			200		1,055		
			300		959		
PET	700–1	Single-step	300	1:1	959	–	(Almazán-Almazán et al., 2010)
	700–4				1,727		
	700–8				1,539		
PET	800–1	Single-step	300	1:1	1,884	–	(Almazán-Almazán et al., 2010)
	800–4				1,971		
	800–8				2,157		
PAN	800–1	Single-step	–	2:1	1,565	0.74	(Chiang et al., 2019)
PS	530–5	800–1	–	3:1	2,562	1.21	(Machado et al., 2021)
Mixed Plastic+ Montmorillonite (1:5)	700–0.2	850–1	–	6:1	1,734	2.44	(Gong et al., 2014)
PVC	1) 300–3 2) 600–2	750–1	100	1:1	400	–	(Kakuta et al., 2009)
				3:1	1,740		
				5:1	550		
PET	500–2	Single-step	–	4:1	353	0.29	(Djahed et al., 2015)
CD and DVD Waste	500–1	700–1	1,800	2:1	1,620	0.78	(Choma et al., 2015)
				4:1	2,710	1.27	
				6:1	2,480	1.17	
PET	1) 520–1 2) 850–1	800–1	–	4:1	2,815	1.45	(Czepirski et al., 2013)
PET	650–4	Single-step	100	6:1	704	–	(Almazán-Almazán et al., 2007)
	800–4				1,023		

(continued on next page)

Table 3 (*continued*)

Precursor	Pyrolysis T/°C – t/ h	Activation T/ °C – t/ h	N_2 Flow Rate mL min^{-1}	Agent/ Precursor ratio	S_{BET} m^2 g^{-1}	Pore Vol. cm^3 g^{-1}	Reference
PAN	920–2.5	Single-step	50	2:1	709	1.00	(Maddah and Nasouri, 2015)
Municipal Plastic Waste	700–0.5	700–1	–	1:1	542	0.24	(Cansado et al., 2022)
PAN	12 %*	Single-step	–	–	1,197	0.54	(Ryu et al., 2000)
	26 %*				2,558	1.28	
	32 %*				3,220	1.80	
PET	850–2	Single-step	–	1:1	1,060	–	(Gómez-Serrano et al., 2021)
				5:1	1,990		
PET	500–0.5	+ Acridine	–	4:1:1	318	0.15	(Arenillas et al., 2005)
		+ Carbazole			418	0.20	
		+ Urea			150	0.10	
PET	600–1	+ Urea 700–1	200	2:1:1	1,209	0.48	(Yuan et al., 2020b)
PAN	280–1.5	+ NaOH 700–2	50	2:1:0.2	2,100	1.01	(Kim et al., 2015)
				3:1:0.1	2,598	1.41	
PAN	1,000–1	KOH 750–3+	100	15 mL/g KOH	1,239	0.43	(Bai et al., 2015)
		HF		200 mL/g HF	1,181	0.39	
		(1 M)+ HF			979	0.31	
		(4 M)					
PET	700 -	+ HNO_3	85	2:1	885	0.31	(Cansado et al., 2010)
		+ NaOH			1,110	0.45	
		+ Urea			1,167	0.46	
Polycarbonate	950–1	600–1	100	4:1	1,123	–	(Méndez-Liñán et al., 2010)
PC				6:1	1,365		
PET	700–0.5	700–1	–	6:1	2,683	1.32	(Zhang et al., 2021)
PVC	600–1	Single-step	–	3:1	1,888	0.76	(Liu et al., 2022)
pre-oxidized with air	800–1				2,507	1.11	
PAN	800–0.5	KOH 800–2	10	4:1:1	3,154	2.11	(Domínguez-Ramos et al.,
pre-oxidized with O_2		+ H_2SO_4			2,764	2.27	2022)

* Burn-off degree.

$K_2O + C \rightarrow 2\ K + CO$(R.9)

$K_2O + H_2 \rightarrow 2\ K + H_2O$(R.10)

Hydroxide dehydrates to form K_2O (R.1), which can react with CO_2 produced by the water-shift reaction (R.3) to form K_2CO_3 (R.4). The removal of these metal salts from carbon during the washing step, along with the structural changes promoted by the activation mechanisms, induces the development of porosity. The metallic potassium resulting from the reactions between the potassium and carbon species (R.5, R.8 and R.9) penetrates the internal structure of the carbon lattice, inducing the generation of the pore network. The formation of physical activating agents such as H_2O (R.1 and R.10) and CO_2 (R.3 and R.6) contributes to the development of porosity by the gasification of carbon (R.2 and R.7). The intermediate potassium compounds, i.e. K_2CO_3 and K_2O, react in the active sites in carbon (R.5, R.8 and R.9), which results in the generation of abundant micropores (>1 nm) (Sun et al., 2017). Thus, the porous structure is developed through the synergistic effect of pore widening, pore combination and pore collapse resulting from the activation mechanisms. These mechanisms are largely dependent on the activation conditions.

Table 3 shows the textural properties of KOH-activated carbons and the activation strategies. A large range of pyrolysis (500–800 °C) and activation (500–900 °C) temperatures is currently used for the preparation of porous carbons treated by potassium hydroxide. The duration is usually 1 or 2 h for each process. According to Lozano-Castelló et al. (2004), the porosity is influenced more by the activation temperature than its duration. De Paula et al. (2018) studied the influence of the activation temperature on the textural properties of polystyrene wastes. Increasing the activation temperature (600–800 °C) enhances the textural properties of the carbon material, manifested by an increment in the S_{BET} (BET specific surface) and pore volume. The largest values were reported for the 800 °C activated carbon: S_{BET} 2,712 m^2g^{-1} and pore volume 1.2 cm^3g^{-1}. Yuan et al. (2020a) obtained porous carbon from PET waste bottles by chemical activation, varying the activation temperature from 700 to 1000 °C. It was found that the S_{BET} and pore volume increased with the increasing activation temperature up to 800 °C and then decreased. The samples activated at 800 °C had the largest S_{BET} and pore volume values of 2,006 m^2g^{-1} and 0.84 cm^3g^{-1}, respectively. The smallest ones were reported for the sample activated at 1000 °C (see Table 3 above). Temperatures over 800 °C are not favourable, since the pore structure can be destroyed (Zhu et al., 2017). This can be due to the sintering and realignment of the carbon structure by the complete decomposition of K_2CO_3, leading to violent gasification (R.6) that partially destroys the pore structure by collapsing or combining the pores (Hock and Zaini, 2018; Ge et al., 2019). Contrariwise, when the temperature is not high enough, the resulting carbon material does not show a well-developed porous structure. No significant chemical changes in the potassium hydroxide occur, since at 500 °C it reacts to form potassium carbonate (R.5) (Illán-Gómez et al., 1996). Consequently, activation temperatures below 500 °C and over 800 °C are not recommended, especially when highly porous carbons are desired. A proper selection of the agent/precursor ratio is also crucial for obtaining activated carbons with the desired textural properties. Typical values range between 1:1 and 4:1 (see Table 3 above). For example, Wang et al. (2009) compared the textural properties of the activated carbons prepared with different agent/precursor ratios, 2:1–4:1, and as precursor they employed polystyrene. The S_{BET} and pore volume increased gradually with the agent/precursor ratio from 1,566 to 2,022 m^2g^{-1} and from 1.05 to 1.35 cm^3g^{-1}, respectively; the conclusion reached was that the larger ratio led to a higher S_{BET} and pore volume. Similarly, Choma et al. (2015) used CDs and DVDs wastes to prepare activated carbons by varying the agent/precursor ratio from 1:1 to 6:1. The S_{BET}, pore volume and micropore volume ranged from 730 to 2,710 m^2g^{-1}, 0.35 to 1.27 cm^3g^{-1}, and 0.32 to 1.15 cm^3g^{-1}, respectively. Those results increased dramatically with the increasing agent/precursor ratio, reaching the maximum at a ratio of 4:1, and then decreased. From the data in Table 3, it can be concluded that increasing the agent/precursor ratio induces a positive trend in the S_{BET} and pore volume. There are two simultaneous mechanisms during the activation process, pore formation and pore widening. By increasing the amount of chemical agent, the extent of the reaction (R.5) increases, and the carbon porosity is developed. The

growing number of chemical species intercalating into the carbon matrix promotes a higher expansion of the pores. However, an excess of pore widening can destroy the pore walls. This may provoke the micropores to coalesce together to form macropores, reducing the specific surface area. According to Huang et al. (2015), if the hydroxide/precursor impregnation ratio is over 6, the pore walls can be degraded, and the porosity of the carbon material reduced. Moreover, impregnation is considered the most polluting stage. A higher ratio leads also to higher costs and longer washing times (Wang et al., 2020a).

It is worth emphasising that the greatest values of S_{BET} and the largest pore volume were obtained for the pre-oxidized activated carbons. Several authors (Shen et al., 2011; Feng et al., 2018; Kamran et al., 2020; Li et al., 2019a, 2019b; Hsiao et al., 2011) pre-oxidized the precursor prior to the carbonization to produce ultra-highly porous carbons. For instance, Li et al. (2019b) claimed to have obtained the largest S_{BET} (3,751 m^2g^{-1}) and the largest pore volume (2.48 cm^3g^{-1}) of all the poly-acrylonitrile-based carbon materials reported in the literature. For that reason, the precursor was mixed first with KNO_3, then subjected to pre-oxidation (240 °C for 2 h) and finally KOH activation (750 °C for 2 h). According to the authors, pre-oxidation of the raw precursor promoted the construction of a semi-carbonized structure, enabling the accessibility of potassium species and leading to an enlargement of the surface area (Li et al., 2019b).

3.1.2. Activation with NaOH

Sodium hydroxide is also a strong and corrosive base that melts without decomposition at 318 °C (Bailar and Trotaman-Dickenson, 1973); it has a lower cost and is less corrosive than potassium hydroxide. Chemical activation using sodium hydroxide proceeds via the same redox reactions as with KOH (Wang and Kaskel, 2012):

$6NaOH + 2C \rightarrow 2Na + 3H_2 + 2Na_2CO_3$ (sSodium hydroxide is consumed at ≈ 700 °C)(R.11).

Thus, the activation mechanisms inducing the development of porosity follow the same considerations as those given for the potassium hydroxide. Table 4 illustrates the preparation and textural properties of NaOH-activated carbons. An under-studied variable affecting the final texture is the flow rate of gas used during the activation treatment. Nitrogen is the most frequently employed gas in chemical activation, which is mostly conducted at a flow rate in the range of 20–200 mL min^{-1} (Tables 3-5). Almazán-Almazán et al. (2010) studied the relationship between the activation parameters and the textural properties of the PET-activated carbons. The hydroxide-impregnated carbon was activated at 100, 200 and 300 cm^3min^{-1}. When the flow rate was increased from 100 to 200 cm^3min^{-1}, there was an increase in both S_{BET} and the micropore volume, from 454 to 1,055 $m^2\ g^{-1}$ and from 0.18 to 0.41 $cm^3\ g^{-1}$, respectively. Another increase up to 300 $cm^3\ min^{-1}$ had almost no impact on these parameters, although an increase in the ultramicropore volume was observed. To understand the influence of the flow rate on the textural properties of these materials, it is necessary to look again at the reactions between hydroxide and carbon during the activation. Reactions 5 and 6 show that several gases evolved during the heat treatment. The faster or slower removal of these gases induced by the N_2 flowing could explain its influence on the development of porosity. According to Lozano-Castelló et al. (2001), when a large flow rate is used, a smaller concentration of these gases is observed. Thus, the gas flow behaves as a purge system. To our knowledge, no more studies have been reported on the influence of the gas flow rate on the textural properties of plastic-based activated carbons. Therefore, further research exploring how the gas flow rate influences the textural properties of these materials is required, especially using gases other than nitrogen. Although the flow rate is an important variable to be controlled in porous carbons production, the impregnation ratio or the heat temperature are the most relevant ones in their final pore characteristics.

3.1.3. Activation with other chemical agents

Table 5 presents the activation conditions under which plastic-based activated carbons are produced using chemical agents other than NaOH and KOH. Among them, phosphoric acid H_3PO_4, zinc chloride $ZnCl_2$, potassium carbonate K_2CO_3 and sulphuric acid H_2SO_4 are the most frequent alternatives to hydroxides. The S_{BET} and total pore volume of H_3PO_4-activated carbons range from 1,223 to 246 $m^2\ g^{-1}$ and from 1.23 to 0.15 $cm^3\ g^{-1}$, respectively (Table 5). Due to the large molecular polarity of H_3PO_4, it is important to control the physical and chemical interactions between the acid and the precursor. Adjusting the concentration of H_3PO_4 solution or the acid/precursor ratio is the primary factor to consider when this agent is used for that purpose. During the activation process, the phosphoric acid reacts with the carbon precursor, leading to the formation of volatile species. The appearance of pores is a direct consequence of the evaporation of these species. However, a high acid/precursor ratio promotes the formation of an isolating layer on the carbon surface, governed by the phosphorus compounds, which inhibits the development of an adequate porosity (Zhong et al., 2012). Moreover, the phosphorus compounds are not easily removed with washing (Liou and Wu, 2009). In the literature reviewed, the most frequent H_3PO_4/precursor ratio was 1:1 (Table 5). On the other hand, activation with phosphoric acid usually requires a lower temperature than the

Table 4
Summary of operating conditions during the activation of plastic material precursors with NaOH and their textural properties.

Precursor	Pyrolysis T/°C - t/ h	Activation T/ °C - t/ h	N_2 Flow Rate mL min^{-1}	Agent/Precursor ratio	S_{BET} $m^2\ g^{-1}$	Pore Vol. $cm^3\ g^{-1}$	Reference
PAN	800–2	800–2	50	2:1	809	0.50	(Singh et al., 2019d)
				3:1	1,020	0.57	
				4:1	967	0.53	
PET	600–1	700–1 1,000–1	200	2:1	1,707	0.80	(Yuan et al. 2020a)
					2,023	1.2	
PU-F	400–1	700–2	60	2:1	710	0.41	(Ge et al., 2019)
PAN pre-oxidized $ZnCl_2$	800–1	Single-step	20	0.8:1	2,012	1.20	(Kamran et al., 2020)
Polycarbonate	500–1.5	Single-step	800	1.5:1	348	–	(Li et al., 2014)
				3:1	756		
Polycarbonate	500–3	Single-step	800	3:1	806	–	(Li et al., 2014)
PET	800–1	Single-step	100	1:1	410	0.86	(Akmil-Başar et al., 2005)
PET	650–1	Single-step	100	6:1	209	–	(Almazán-Almazán et al., 2007)
	650–4				269		
	650–8				337		
PET	800–0.5	Single-step	100	2:1	770	–	(Marzec et al., 1999)

Table 5
Summary of the activation conditions of plastic precursors with several chemical agents and their textural properties.

Chemical Agent	Precursor	Pyrolysis T/ °C – t/ h	Activation T/ °C – t/ h	N_2 Flow Rate mL min^{-1}	Agent/Precursor ratio	S_{BET} m^2g^{-1}	Pore Vol. cm^3 g^{-1}	Reference
Melamine + $ZnCl_2$/ NaCl	PET	450–0.13 550–0.13	Single-step	–	0.5:2:1	612 1,173	–	(Song et al., 2020)
$NaNH_2$	PAN	800–2	800–2	50	2:1 3:1 4:1	549 833 803	0.29 0.36 0.34	(Singh et al., 2019d)
K_2CO_3	PAN	800; 2	800–2	50	2:1 3:1 4:1	1,110 1,250 846	0.50 0.64 0.44	(Singh et al., 2019d)
$Ca(OH)_2$	PU-F	400–1	700–2	60	2:1	39	0.04	(Ge et al., 2019)
$ZnCl_2$	PAN	700–0.5	Single-step	–	4:1	1,074	0.49	(Tsuchiya et al., 2021)
H_3PO_4 H_2SO_4 $ZnCl_2$	PET	1) 400–1 2) 800–1	Single-step	50	1:1	1,223 583 682	0.73 0.37 0.47	(Adibfar et al., 2014)
H_2SO_4	PET	600–0.5	Single-step	100	2:3	536	0.36	(Sureshkumar and Susmita, 2018)
K_2CO_3	PU-F	800–1	Single-step	400	1:1 1:10	2,772 1,566	– 	(Hayashi et al., 2005)
H_2SO_4	PET	800–1	Single-step	–	1:3	420	0.36	(Kartel et al., 2001)
K_2CO_3 KNO_3	PAN	800–1	Single-step	20	0.8:1	1,179 971	0.54 0.45	(Kamran et al., 2020)
H_2SO_4	PET	500–1 800–1	Single-step	100	1:1	610 1,030	0.15 0.60	(Kartel et al., 2006)
H_3PO_4	PET	600–0.5	Single-step	–	3:1	683	–	(Cansado et al., 2008)
$FeCl_3$	PET	500–2	Single-step	–	–	402	–	(Marzec et al., 1999)
CaO + MgO	PET	850–1	Single-step	–	1:5 2.5:1	331 106	–	(Przepiórski et al., 2013)
H_3PO_4	PET	450–4	Single-step	–	1:1	261	0.15	(Ahangar et al., 2021)
H_3PO_4	Kevlar	700–1	Single-step	80	1:3	403	0.21	(Giraldo et al., 2007)
K_2CO_3	Plastic Fuel	900–2 500–2	Single-step 900–2	500	1:1	310 1,300	–	(Kadirova et al., 2006)
K_2CO_3	Municipal plastic waste	700–0.5	700–1	–	1:1	623	0.25	(Cansado et al., 2022)
$ZnCl_2$	PET	500–2	Single-step	100	1:1	700	0.69	(de Castro et al., 2018)
K_2CO_3	PET	800–2	Single-step	100	1:4 1:1	680 1,390	0.69 1,55	(de Castro et al., 2018)

hydroxides. H_3PO_4 promotes the dehydration of the carbon precursor and can act as a catalyst, enabling the release of physical agents such as CO and CO_2, which react with carbon at a lower temperature (Jagtoyen and Derbyshire, 1998). When the hydroxides are used (R.1), these mechanisms occur at higher temperatures. Thus, a lower activation temperature is required when using this chemical agent. For the carbon materials derived from precursors of a different nature, there are also reports on the S_{BET} and pore volume decreasing as the agent ratio and temperature increase (Attia et al., 2008; Benadjemia et al., 2011, Kang et al., 2018 Khamkeaw et al., 2019).

Zinc chloride is another chemical agent used for inducing porosity in the plastic-based carbons. The S_{BET} and the total pore volume of $ZnCl_2$-activated carbons range from 1,439 to 682 m^2g^{-1} and from 0.7 to 0.47 cm^3g^{-1}, respectively (Table 5). In contrast to the previous agent, the textural characteristics of $ZnCl_2$-activated carbons are favoured by increasing the amount of this agent. In fact, the highest textural values were obtained for the sample activated with the largest agent ratio (Table 5). During the thermal treatment, volatile species are released from the carbon, creating cavities on its surface. Zinc chloride enables the movement of those species by preventing the formation of compounds that can block the surface. Thus, increasing the mass ratio of $ZnCl_2$ promotes the release of those species, enhancing the N_2 adsorption (Arami-Niya et al., 2010). Moreover, the porosity increment is also accomplished via the appearance of pores left by $ZnCl_2$ after the washing step. Concerning the activation temperature, this agent usually requires a lower activation temperature than with hydroxides. During the activation, $ZnCl_2$ promotes the formation of cross-linking structures with a low thermal stability (Kong et al., 2017). At temperatures over 500 °C, the breakdown and rearrangements of carbon aggregates occur, leading to collapse of the pores. Moreover, this agent might also act as a dehydrator.

The S_{BET} and the total pore volume of K_2CO_3-activated carbons range from 2,772 to 310 m^2g^{-1} and from 0.64 to 0.44 cm^3g^{-1}, respectively (Table 5). During the heat treatment, the main reactions taking place between K_2CO_3 and the carbon species are shown in the previous section (R.6, R.8 and R.9). As mentioned above, the development of porosity is mainly attributed to the reduction of K_2CO_3 by carbon to form K, K_2O, CO_2 and CO. The resulting potassium species can intercalate into the carbon lattice, widening the existing pores. The carbon gasification also contributes to expansion of the pores. Moreover, new cavities are produced on the carbon surface when those compounds are evaporated (Liu et al., 2015 Wang and Kaskel, 2012). K_2CO_3 being an intermediate species formed during the KOH-activation, similar considerations can be given to both chemical agents.

Concerning the H_2SO_4-activated carbons, the S_{BET} and the total pore volume range from 1,030 to 420 m^2g^{-1} and from 0.60 to 0.36 cm^3g^{-1}, respectively (Table 5). H_2SO_4 promotes the partial degradation of the carbon precursor chiefly via the dehydration reactions. During the

activation, sulphuric acid penetrates the carbon matrix, developing a large or medium porosity on the carbon surface. Given that this activator can dissolve many impurities from carbon precursors, it can also be used as a cleaning or de-ashing agent for carbon precursors (Cheng et al., 2016).

Other chemical agents such as $Ca(OH)_2$, HNO_3 or $FeCl_3$ were also used to produce porous carbons. However, the literature proves that their use to activate plastic waste is very limited compared to the chemical agents discussed above. Moreover, the activation with these agents usually induces less porosity in the resulting material (Table 5).

An interesting issue is the comparison between single-step and two-step chemical activation. Kadirova et al. (2006) prepared activated carbons by chemical activation using the single-step and two-step methods. The raw plastic waste was impregnated in K_2CO_3 (2:1) and directly activated at 900 °C in the single-step method. However, for the two-step method, the precursor was first carbonized at 500 °C and subsequently activated at 900 °C. The S_{BET} value of the single-step-activated carbon was 310 m^2g^{-1}, and for the two-step-activated carbon was 1,300 m^2g^{-1}. Similar findings can be drawn from a comparison of the papers by Singh et al. (2019b) and Maddah and Nasouri (2015) in Tables 3-4. The two-step method is also more favourable in terms of the development of porosity when using hydroxides as activators. In the direct method, the agent is concentrated chiefly on the surface and the interior carbon matrix hardly reacts. Nevertheless, carbonization prior to the activation enables the formation of fine cavities, creating accessible pathways toward the active sites within the carbon structure. Therefore, more chemical species can react with the carbon compounds, increasing the reaction rate (Saad et al., 2019). The result is a larger specific surface area and pore volume; however, the two-step method is more energy-consuming.

To sum up, the literature reviewed in this study discusses the variables affecting the development of porosity in chemically activated carbons. The textural characteristics can be tuned by the appropriate control of those variables. KOH is the preferred agent for the preparation of porous carbon from plastic waste precursors due to its major role in the enhancement of the textural properties (surface areas up to 3,800 m^2g^{-1} and pore volume up to 2.5 cm^3g^{-1} (Li et al., 2019b)). In comparison, NaOH is a less effective activator, but costs less and is more environmentally friendly as well as less harmful than KOH. Both hydroxides act as oxidants. K_2CO_3 is also a non-hazardous and effective activator in preparing porous carbons with nicely controlled structures. $ZnCl_2$ and H_3PO_4 serve as dehydrating agents, so a lower activation temperature is usually required. The former is toxic, with a more-polluting character than the latter. Once the agent is selected, the impregnation rate and the activation temperature were found to be the most relevant parameters in the activation process. As shown below, the attractive features of the chemically activated materials, such as a large surface area and abundant micropores, make them powerful candidates for application in the field of CO_2 capture.

3.2. Effects under physical activation conditions

Physical activation is considered to be a green method for activated carbon preparation because it is chemical-free (Pallarés et al., 2018); it is also simpler than chemical activation, and consequently, fewer parameters are to be controlled in this type of activation. For the activation of plastic-based char, the most frequently used activating agents are carbon dioxide and steam, although some authors also used air or their binary mixture. These media can have different effects on the formation of porous carbon. Physical activation is a controlled gasification where partial or total oxidation of char is governed by the oxidizing atmosphere. Carbon dioxide and steam react endothermically with the carbon species according to the following reactions (Liu et al., 2020):

$C + CO_2 \leftrightarrow 2CO$ ($\Delta H = 159.0$ kJ/mol)(R.12).

$C + H_2O \leftrightarrow CO + H_2$ ($\Delta H = 118.5$ kJ/mol)(R.13).

During these reactions, carbon species undergo chemical degradation by selective oxidation, the most reactive species being the first to be removed. These carbon species are converted into carbon monoxide and released in gaseous form. For the development of suitable porosity, the removal of carbon atoms should occur dominantly into the carbon matrix instead of its surface. In this way, the gas is released from a deeper level, and the formation and widening of pores are more pronounced. The development of porosity is governed by these removal processes, which are manifested by the carbon material weight loss (Rodríguez-Reinoso et al., 1995).

The degree of activation is usually referred to as the burn-off value, which is the difference between the masses before (carbon) and after (activated carbon) the activation:

$$\text{Burn} - \text{off}(\%) = \left(\frac{W_0 - W}{W}\right)100$$

where W_0 is the initial mass of the carbonized sample and W refers to the final mass after the activation.

Table 6 compiles the textural properties of physically activated carbons derived from plastic wastes and the activating strategies. The main factors controlling the activation process are the physical agent, activation temperature, holding time and burn-off.

3.2.1. Activation with CO_2

Table 6 shows that porous carbons with large surface areas (the maximum S_{BET} values in the range of 2,000–2,800 m^2g^{-1}) can be obtained by CO_2 physical activation. Generally, physical activation is conducted at 700–1,000 °C, which is a higher range of temperatures than that used for chemical activation. Kumar et al. (2018) prepared porous carbons from styrene acrylonitrile wastes by physical activation in CO_2 atmosphere at 700, 800 and 900 °C. The S_{BET} increased from 497 to 1,358 m^2g^{-1} when the activation temperature changed from 700 to 900 °C. A similar trend was observed for the pore volume values. Hong et al. (2016) also studied the influence of temperature on the textural properties of polyvinylidene fluoride-activated carbons. The precursor was activated in the range of 700–950 °C in CO_2 atmosphere for 1 h. The S_{BET} and pore volume were clearly enhanced by increasing the activation temperature. The highest S_{BET} and pore volume values of 2,750 m^2g^{-1} and 1.46 cm^3g^{-1} were reported for the sample activated at 950 °C. The burn-off value increased proportionally with the increasing activation temperature, exhibiting a linear correlation between the textural parameters and the burn-off values. CO_2 activation involves the C-CO_2 reaction, which results in the removal of carbon species (R.12). The active sites determine the progress of carbon removal. Further temperature increment promotes the migration of CO_2 along the existing pores to approach the active sites for reaction. The active oxygen of the physical agent promotes the openness of the block pores, the formation of new ones and their expansion by burning the carbonization off-products, which are trapped within the carbon structure (Sevilla and Mokaya, 2014). Hence, an increment of the activation temperature contributes to the carbon particle removal, which is manifested by a higher burn-off value. Consequently, a porous structure is gradually formed, during which CO and CO_2 are released.

In contrast to chemical activation, the porosity of the physically activated carbons is greatly influenced by the activation time. This can be seen in Table 6, where a wide range of activation times (0.5–72 h) is found. Belo et al. (2017) prepared porous carbons from PAN wastes by physical activation with CO_2 at 800 °C. To study the influence of the activation time, the PAN activation was conducted ranging from 4 to 20 h. The S_{BET} and pore volume increased from 322 to 1,230 m^2g^{-1} and from 0.14 to 0.56 cm^3g^{-1}, respectively. The thermogravimetric analysis showed that the burn-off evolution was closely related to the activation time. Moura et al. (2018) obtained porous carbons by CO_2 activation of pyrolyzed PET waste. The samples were activated at 925 °C for 24, 36

Table 6
Summary of operating conditions during the physical activation of plastic material precursors and their textural properties.

Physical Agent	Precursor	Pyrolysis T/ºC – t/ h	Activation T/ ºC – t/ h	Flow Rate mL min^{-1}	S_{BET} $m^2 g^{-1}$	Pore Vol. $cm^3 g^{-1}$	Reference
Air	High-density polyethylene HDPE	Fast pyrolysis 450	900–3	–	16.77	0.20	(Jamradloedluk and Lertsatitthanakorn, 2014)
CO_2	PU-F	400–1	800–2	15	15	0.04	(Ge et al., 2019)
			900–2		206	0.10	
			1,000–2		865	0.42	
CO_2	Styrene Acrylonitrile SAN	700–0.25	700–3	1,000	497	0.13	(Kumar et al., 2018)
		900–0.25	900–3		1,358	0.19	
CO_2	PET	800–1	800–2	110	696	0.24	(Belo et al., 2017)
			800–8		1,400	0.46	
CO_2	PAN	800–1	800–4	110	322	0.14	(Belo et al., 2017)
			800–20		1,230	0.56	
CO_2	Kevlar	560–0.5	750–4	300	630	–	(Conte et al., 2020)
				900	752		
CO_2	Kevlar	550–0.5	700–5	300	923	0.44	(Choma et al. 2016)
			750–3		1,240	0.61	
			800–1		737	0.38	
Steam + N_2 (85:15)	Tyre	450 -	975–2	700	350	0.46	(Hadi et al., 2016)
			975–6		732	0.91	
CO_2	PET	825–1.5	900–8	170	1,210	–	(Bratek et al., 2013)
			940–5		1,830		
Steam + N_2 (60:100)	PVC	900–1.5	900–0.5	200	1,096	0.72	(Qiao et al., 2004)
			900–1.5		2,096	1.34	
Steam + N_2 (1:1)	PET	750–0.5	900–1.5	–	1,170	0.62	(Laszlo and Szucs, 2001)
Steam	PET	500 -	900–78 %*	200	1,700	0.15	(Nakagawa et al., 2000)
Steam + N_2 (50:50)	PAN	750–0.5	900–50 %*	800	544	0.28	(László et al., 2000)
	PET				1,190	0.62	
Steam	PET	500–1	850–2	200	1,450	–	(Nakagawa et al., 2003)
			850–4		1,740		
CO_2	PET	800–1	950 – 4	100	438	0.24	(Esfandiari et al., 2012)
			1,000 – 4		851	0.46	
CO_2	Polyvinylidene fluoride	800–1	Single-step	200	1,479	0.62	(Hong et al., 2016)
	PDF	950–1			2,750	1.46	
N_2	PDF	400–2	Single-step	–	245	0.14	(Lee and Park, 2014)
		600–2			995	0.49	
CO_2	PET	800–1	975–4	–	2,010	0.93	(Esfandiari et al., 2011)
Steam + N_2 1:1	PET	750–1.5	900–1.5	300	1,443	0.70	(Podkościelny and László, 2007)
CO_2	PET	950–1	950–4	100	1,367	–	(Fernández-Morales et al., 2005)
			950–8		1,914		
Steam	PET	500–1	850–1	200	1,200	–	(Nakagawa et al., 2004)
	PET + $Ca(NO_3)_2$				1,200		
CO_2	PET	925–2	925–24	10	984	0.40	(Moura et al., 2018)
			925–36		1,351	0.58	
			925–72		2,176	1.03	
CO_2 and N_2	PET	1) 400–1	1) N_2 925–1	10	659	0.36	(Rai and Singh, 2018)
		2) 725–2	1) CO_2 925–2				
Steam	PET + Act. H_2SO_4	800–0.5	Single-step	–	1,030	0.81	(Sych et al. 2006)
Steam + N_2 1:1	PET	700 -	900–1.5	300	1,190	0.42	(Bóta et al., 1997)
Steam	PET	900–1	Single-step	–	1,061	–	(Gómez-Serrano et al., 2021)
Self-generated atmosphere	PET	200–0.25	700–5	–	515	0.54	(Collin et al., 2016)
Steam	PAN	7.5 %*	Single-step	–	749	0.32	(Ryu et al., 2000)
		12 %*			1,241	1.10	
Air	PAN	3.9 %*	Single-step	–	384	0.17	(Ryu et al., 2000)
		5.3 %*			527	0.23	
Air	Municipal Plastic Waste	700–0.5	700–1	–	318	0.17	(Cansado et al., 2022)
CO_2	Kevlar	900–3.5	800–12 %*	40	543	0.29	(Martínez-Alonso et al., 1997)
			800–65 %*		986	0.50	
Steam	Kevlar	900–3.5	850–1	50	458	0.24	(Giraldo et al., 2007)
CO_2	Waste Cds and DVDs	500–1	920–1	25	390	0.18	(Choma et al. 2014)
			920–5		1,560	0.77	
			920–8		2,440	1.36	
Steam CO_2	PET	1) 520–1	800–50 %*	–	1,042	0.47	(Czepirski et al., 2013)
		2) 850–1	850–50 %*		1,122	0.52	
Steam	PS	900–3	900–0.75	–	1,555	1.29	(Wang et al., 2009)
	Plastic Fuel			500		–	(Kadirova et al., 2006)

(*continued on next page*)

Table 6 (*continued*)

Physical Agent	Precursor	Pyrolysis T/°C – t/ h	Activation T/ °C – t/ h	Flow Rate mL min^{-1}	S_{BET} $m^2 g^{-1}$	Pore Vol. $cm^3 g^{-1}$	Reference
Steam/N_2		900–2	Single-step		282		
80:20		500–2	900–2		420		
Steam	Municipal Plastic waste	350–8	850–5	200	378	–	
	M. Plastic w. + HNO_3				828		(Nagano et al., 2000)
CO_2	PET	725–2	925–12 %*	10	668	–	(Parra et al., 2006)
			925–35 %*		1,405		
			925–76 %*		2,468		
Ar	Poly(vinylidenefluoride)	500–2	Single-step	500	880	0.41	
	PVDF	900–2			1,037	0.47	(Park et al., 2020)
CO_2	PVDF	500–2	Single-step	500	856	0.41	(Park et al., 2020)
		900–2			1,158	0.53	
Steam	PET + Act. H_2SO_4	800–1	800–1	–	1,230	0.54	(Kartel et al., 2001)
CO_2	PET	400–4	975–1	200	1,591	–	(Yuliusman et al., 2017)
CO_2	Plastic Box Waste	700–0.5	800–5	–	701	0.25	(Cansado et al., 2022)
CO_2	PET	925–38 %*	Single step	–	1,426	0.58	(Mestre et al., 2009)
CO_2	Tyre	800–1	750–3	600	126	–	(González et al., 2006)
			850–3		496		
Steam/N_2	Tyre	800–1	750–2	600	213	–	(González et al., 2006)
85:15			900–2		1,317		
CO_2	Polycarbonate	950–1	950–1	100	656	–	(Méndez-Liñán et al., 2010)
			950–8		1,927		

*burn-off degree.

and 72 h. The burn-off degrees after 24, 36 and 72 h of activation were 22 %, 41 % and 76 %, respectively, showing a strong correlation between both variables. The greatest textural parameters were reported for the 72 h activated sample. Another common practice for activated carbon preparation is setting the burn-off degree instead of the activation time. For instance, Mestre et al. (2009) prepared a series of porous carbons from PET by physical activation with CO_2 at 925 °C. The samples were activated until burn-off degrees of 12 %, 35 %, 58 % and 76 % were reached. It was observed that the samples developed a better porosity with the increasing burn-off degree. A general trend is that all the S_{BET}, pore volume and micropore volume values increase with the increase of the burn-off value (weight loss). In turn, the burn-off degree depends on both the temperature and activation time. Consequently, the higher the activation temperature or the longer the activation time, the greater the porosity.

3.2.2. Activation with steam

Steam is another common agent used for the preparation of physically activated carbons. The porosity is developed chiefly through the extensive reaction between the steam and the carbon species (R.13). Steam is a more reactive agent than carbon dioxide, causing a faster reaction (higher reaction rate) with the carbon species (Rodríguez-Reinoso et al., 1995). Thus, the activation of plastic wastes with steam usually requires the application of lower temperatures (500–900 °C). González et al. (2006) carbonized tyre wastes prior to steam and CO_2 activation and discussed the effects of both agents on the resulting textural properties. The samples were activated in the range of 750–900 °C for 1–3 h. The steam gasification produced greater N_2 adsorption, which was manifested by higher values of S_{BET} and pore volume than the CO_2 samples. For instance, the S_{BET} and pore volume for the steam- and CO_2-samples activated at 850 °C for 3 h were 872–496 m^2g^{-1} and 0.33–0.20 cm^3g^{-1}, respectively. The N_2 adsorption isotherms showed that the CO_2 activation required 50 °C more to match the porosity of the steam sample. Moreover, the burn-off degree of the samples was 77 % (steam) and 60 % (CO_2), showing that steam is a more reactive agent than CO_2 and requires lower activation temperatures. This fact was also reported by other authors using precursors of different natures (Ioannidou and Zabaniotou, 2007).

As follows from Table 6, some authors used a mixture of different gaseous agents to produce activated carbon. For instance, László et al. (2000) used PET wastes to obtain porous carbon by gasification under a mixed atmosphere of N_2 + steam (1:1). The precursor was firstly carbonized at 750 °C for 0.5 h and then subjected to gasification at 900 °C for 1.5 h. The S_{BET} and pore volume values increased from 242 m^2g^{-1} and 0.14 cm^3g^{-1} (carbonized PET) to 1,190 m^2g^{-1} and 0.62 cm^3g^{-1} (activated PET). This indicates that the gasification in a mixed medium can also be effective to prepare porous carbon materials. Nitrogen is combined with steam because the latter can react with the carbon species with a high reaction rate. The addition of nitrogen slows down the carbon conversion into gas and facilitates the control of the burn-off degree. In contrast, CO_2 is not mixed with nitrogen since the reaction of CO_2 with the carbon species is substantially slower.

Although mixing the gas agents is intended to achieve a synergistic effect of each gas, the contrary effect can also take place. For instance, the activation by the binary mixture of CO_2 and steam can include two possible reaction mechanisms: the carbon-CO_2 and carbon-H_2O reactions (R.11 and R.12) occur at the same reactive sites, competing between themselves, which can result in a lower reaction rate (Chen et al., 2013). In the other case, these reactions occur at different sites, inducing a larger degradation in the carbon structure, which enables the agent diffusivity. This results in an increment of the reaction rate and a better porosity is developed (Guizani et al., 2016). The mechanisms occurring in the mixed atmospheres are more complicated to explain than those of the pure atmosphere. To our knowledge, there are no studies dealing with the influence of different gas compositions on the textural properties of the carbons derived from plastic wastes. Thus, further research should be carried out to understand how the gasifier design can influence the resulting textural properties of these materials.

3.2.3. Activation with other physical agents

In addition to the common physical agents, porous carbon can also be prepared using other gasifiers (e.g., air, argon, or nitrogen). However, there are few studies on the activation of plastic wastes under these atmospheres. Ryu et al. (2000) prepared PAN-porous carbon with various degrees of activation by air gasification. The S_{BET} values for the samples with 3.9 % and 5.3 % activation degrees were 384 and 527 m^2g^{-1}, while those of the pore volume were 0.17 and 0.23 cm^3g^{-1}, respectively. The air gasification induced the development of large porosity in the resulting carbon material, even working at small activation degrees, which is attributed to the high oxidant character of the

O_2 in the air. However, high reactivity of O_2 hinders the control of the burn-off degree, which is not favourable for tailoring the porosity characteristics of the resulting material (Benedetti et al., 2017). Park et al. (2020) obtained porous carbon from PVDF wastes by argon and CO_2 gasification, and proved that the resulting porous carbon developed a similar porosity, which indicates that argon can also be considered to be an efficient agent (Table 6).

Physical and chemical activations can also be combined to produce activated carbons with well-developed porosity. This hybrid method begins with chemical activation followed by physical activation. Its purpose is to reach the synergistic effect of each activation on the resulting material properties. Sych et al. (2006) used this method and prepared porous carbon from PET wastes, including chemical activation with H_2SO_4 followed by physical activation with steam. It was found that this allowed for the development of large porosity in a much shorter time than physical activation only. Combined activation needed 5 min to reach 70 % of the burn-off degree, while physical activation usually takes 1.5 h under the same conditions (László, 2005; Laszlo and Szucs, 2001). Kartel et al. (2006) also used hybrid activation to obtain porous carbons from PET wastes. They considered this activation to be an express-activation method due to the shorter activation time required to obtain large burn-off values. Moreover, the authors claimed that a lower activation temperature is needed when employing the combined activation. This proves that hybrid or combined activation is also an effective method to produce porous carbons, improving the technological procedure and resulting in a significant energy saving.

According to the literature review, physically activated carbons derived from plastic wastes have well developed surface areas and pore volumes ranging from 15 to 2,750 m^2g^{-1} and 0.04 to 1.46 cm^3g^{-1}, respectively. From the data collected in Tables 3-6, it is possible to state that the physically activated carbons develop a smaller surface area and pore volume than the chemical ones. Compared to physical activation, chemical activation provided activated carbons with a more porous structure than those obtained using physical activation (Cui et al., 2011). However, one of the main weaknesses of this routine is the need for repeated washing steps to remove the residual chemical activating agent from the final solid. Moreover, appropriate treatment is required for the toxic wastewater produced in the washing step (Wang et al., 2016). On the other hand, chemical activation requires a lower activation temperature (500–800 vs. 700–1,000 °C) and time (1–2 vs. 3–10 h). The long activation time and small adsorption capacity of the prepared activated carbon along with its large energy consumption are the main disadvantages of the physical activation methods (Yahya et al., 2015). Another important advantage of the chemical activation method is that it provides a better control of the development of porosity, which is specifically important for the synthesis of any effective CO_2 adsorbent material. However, physical activation is simpler, cheaper, and more favourable in terms of environmental safety. Consequently, the carbon-based materials characterized by great performance in terms of textural properties should have the potential to be studied for their CO_2 adsorption capacity. The next section will estimate this.

4. Application of plastic-based activated carbons for co_2 capture

Numerous studies have described the successful conversion of plastic wastes into activated porous carbon for different applications, such as supercapacitors (Sevilla and Mokaya, 2014), catalysis (Calvino-Casilda et al., 2010), removal of pollutants from wastewater (Wang et al., 2021), hydrogen storage (Gong et al., 2014), etc. However, fewer studies consider their application as CO_2 adsorbents. It is well known that there is a close correlation between the CO_2 adsorption capacity of the activated carbons and their textural properties; however, there are different views concerning which textural parameter dominates the CO_2 adsorption capacity. This section summarizes some of the main results found in the literature on this issue, which could allow relevant conclusions to be extracted. Table 7 displays the textural parameters - specific surface and micropore volume -, and the adsorption capacities of precursors obtained from wastes of some frequently used plastics. It shows the nature of the type of activation - chemical/physical - as well as the activation conditions used for the preparation of activated carbon.

4.1. CO_2 adsorption capacity of chemically activated carbons

As shown in Table 7, chemically activated carbons prepared from plastic wastes can achieve, or even exceed, the CO_2 adsorption capacity of commercial adsorbents. For instance, their adsorption capacity at low temperatures (<10 °C) ranged from 8.93 to 1.99 mmol g^{-1} (1 atm). It is worth noting that the adsorption mechanism is strongly influenced by the process temperature. Most of the adsorbents showed a decreased adsorption capacity as the temperature increased. The adsorption capacities at medium (20–50 °C) and high (75–100 °C) temperatures ranged between 4.9 and 0.92 and 1.35–0.28 mmol g^{-1}, respectively (1 atm). The increase in the molecular kinetic energy of the gaseous species at higher temperatures is the well-known reason for this phenomenon (Kamran et al., 2020).

The selection of an appropriate precursor for the production of activated carbons considerably influences their adsorption capacity. PET plastic wastes can be considered suitable precursors to produce efficient CO_2 adsorbents due to their large carbon (over 60 wt%) and oxygen contents (Lian et al., 2011). For instance, Yuan et al. (2020a) prepared activated carbons from PET plastic bottles using KOH and NaOH and evaluated their CO_2 adsorption capacities. The activation was conducted at different temperatures (700–1,000 °C). The KOH- and NaOH-samples activated at 700 °C exhibited the largest CO_2 uptake of 4.42 and 3.86 mmol g^{-1}, respectively. For both chemicals used in the activation process, the CO_2 capture capacity was gradually reduced by increasing the activation temperature. The authors reported that a high activation temperature was not favourable to develop narrow micropores (<0.8 nm), which was the main governing mechanism in the CO_2 adsorption process. Adibfar et al. (2014) studied the CO_2 adsorption capacity of chemically activated PET wastes using KOH, H_3PO_4, $ZnCl_2$ and H_2SO_4 as chemical agents. It was reported that the KOH-activated carbon was the most efficient adsorbent, which was manifested by the largest adsorbed amount of CO_2 (3.5 mmol g^{-1} at 25 °C and 1 atm). The sequence of the CO_2 adsorption capacity of the samples was: KOH > H_3PO_4 > $ZnCl_2$ > H_2SO_4. The same trend was found for the surface area and pores volume. Lian et al. (2011) compared the physicochemical characteristics of the activated carbons derived from different starting materials, i.e., PVC and PET. The PET-activated carbon exhibited the best pore characteristics, which was mainly explained by the aromatic structure of the PET polymer. The authors stated that the PET precursor is more suitable to develop efficient adsorbents than the PVC one. Kaur et al. (2019b) studied the influence of the activation conditions on the CO_2 adsorption capacity and found that the largest adsorption capacity was achieved for the sample activated at 700 °C for 2 h with the 3:1 KOH/precursor ratio, owing to its well-developed pore system.

Carbonized waste polyurethane was studied by Ge et al. (2016), using KOH as a chemical activation agent. It exhibited a considerable performance for the CO_2 uptake, with a capacity of 6.67 and 4.33 mmol g^{-1} at 0 and 25 °C, respectively. According to these authors, the highest adsorption capacity corresponded to the largest ultramicropore volume. Kevlar waste was studied by Choma et al. (2014). They prepared chemically activated carbons and studied their CO_2 adsorption behaviour. The activation was conducted by varying the KOH/precursor ratio. All samples increased their adsorption capacity with the increasing KOH ratio in the range of 1–4, and it then dropped with the further increase of KOH. The authors reported that the amount of CO_2 adsorbed was correlated with the micropore volume. The largest adsorption capacity of 4.47 mmol g^{-1} was reported for the sample impregnated at the KOH ratio of 4:1. The importance of developing narrow microporous structures for efficient CO_2 capture has been an issue considered in most reports found in the literature on this topic. Sevilla and Fuertes (2011)

Table 7
Summary of CO_2 adsorption and textural properties of plastic-based activated carbons.

Precursor	Activation	Ads. Conditions T/ °C	Ads. conditions P/ atm	Ads. Capacity mmol g^{-1}	S_{BET} m^2 g^{-1}	Micropore cm^3 g^{-1}	Narrowp. cm^3 g^{-1}	Reference
PAN	$NaNH_2$	30	1	1.75	833	0.34	–	(Singh et al., 2019d)
	NaOH			2.20	1,020	0.51		
	K_2CO_3			2.44	1,250	0.57		
	3:1 – 800° –2							
PAN	KOH	30	–	1.2	1,890	0.99	–	(Singh et al., 2019b)
	3:1 – 800° –2	50		0.92				
PAN	KOH	30	1	2.5	1,884	0.92	–	(Singh et al., 2019c)
	3:1 – 800° –2	75		1.3				
PET	KOH	25	1	4.42	1,812	0.71	0.37	(Yuan et al. 2020a)
	2:1 – 700° –1	75		1.35				
PET	NaOH	25	1	3.86	1,707	0.70	0.34	(Yuan et al. 2020a)
	2:1 – 700° –1	75		1.25				
PET	MgO/CaO	20	1	0.22	106	0.22	–	(Przepiórski et al., 2013)
	2.5:1 – 850° –1	70		0.28				
PU-F	KOH	0	1	6.67	1,516	0.57	0.18	
	1:1 – 700° –1	25		4.33				(Ge et al., 2016)
	KOH			5.85	1,360	0.52		(Ge et al., 2019)
PU-F	NaOHCa	0	1	4.12	710	0.20	–	
	$(OH)_2$			1.99	39	0.01		
	2:1 – 700° –2							
Kevlar	KOH	0	1	4.47	2,660	1.35	0.85	(Choma et al. 2014)
	4:1 – 700° –0.5			4.27	2,450	1.23	0.87	
	5:1 – 700° –0.5							
Waste CDs and DVDs	KOH	0	1	5.8	2,710	1.15	0.68	(Choma et al. 2015)
	4:1 – 700° –1	25		3.3				
PET	KOH	20	1	2.2*	472	–	–	(Arenillas et al., 2005)
	+ Acridine			2.9*	318			
	+ Carbazole			4.8*	418			
	+Urea			2.7*	150			
	4:1:1 500–0.5							
PET	KOH	25	1	3.5	1,338	0.61	–	(Adibfar et al., 2014)
	H_3PO_4			3.1	1,223	0.55		
	$ZnCl_2$			2.3	682	0.34		
	H_2SO_4			1.8	583	0.29		
	1:1 800–1							
PAN	KOH+ HF	–	1	0.76	1,239	0.42	–	(Bai et al., 2015)
	(4 M)			1.61	979	0.21		
	15 mL/g 750–3							
PAN	KOH	0	1	5.6	3,072	1.16	1.75	(Kamran et al., 2020)
	NaOH			5.8	2,012	0.82	1.20	
	KNO_3			3.3	971	0.39	0.45	
	K_2CO_3			4.2	1,179	0.46	0.54	
	0.8:1 800–1							
PAN	KOH	50	1	2.70	2,366	0.45	–	(Hsiao et al., 2011)
	3:1 900–3.5							
PAN	KOH	25	1	2.74	1,565	0.50	0.20	(Chiang et al., 2019)
	2:1 800–1	55		1.38				
Mixed Plastic	KOH	40	1	0.57	1,734	–	–	(Gong et al., 2014)
	pre-treated with Montmorillonite		10	6.75				
	6:1 850–1		45	18.1				
PET	KOH + Urea	0	1	6.23	1,165	0.46	–	(Yuan et al., 2020b)
	1:2:1 700–1	25		4.58				
		50		2.82				
PAN	KOH + NaOH	0	1	6.84				(Kim et al., 2015)
	2:1 + 20 % 700–2	25		4.98	2,100	0.93	0.35	
PET	Melamine + $ZnCl_2$/NaCl	0	1	6.47	1,173	–	–	(Song et al., 2020)
	2:1 550–0.13	25		4.67				
PET	KOH	30	1	2.31	1,690	0.78	–	(Kaur et al., 2019b)
	3:1 700–2	50		1.35				
PAN	KOH	25	1	3,11	780	0.35	–	(Shen et al., 2011)
	pre-oxidized with air			4,42	2,231	0.76		
	2:1 850–1							
PVC	KOH	0	1	6.9	2,453	0.91	0.37	(Liu et al., 2022)
	pre-oxidized with air	25		3.9				
	3:1 700–3							
PVC	KOH	0	1	8.93	2,453	0.91	0.37	(Wang et al., 2020b)
	pre-oxidized with NaOH, TBD, Ethanol	25		5.47				
	3:1 500–700 – 3							

(*continued on next page*)

Table 7 (*continued*)

Precursor	Activation	Ads. Conditions T/ °C	P/ atm	Ads. Capacity mmol g^{-1}	S_{BET} m^2 g^{-1}	Micropore cm^3 g^{-1}	Narrowp. cm^3 g^{-1}	Reference
PAN	KOH 4:1 800–2	0	1	0.91	3,154	0.54	–	(Domínguez-Ramos et al., 2022)
Kevlar	CO_2 700° −5 750° −3	0	1	4.88 6.58	923 1,240	0.41 0.54	0.34 0.44	(Choma et al. 2016)
PU-F	CO_2 800° −2 900–2	0	1	2.4 3.2	15 206	0.03 0.08	–	(Ge et al., 2019)
Waste CDs and DVDs	CO_2 920° −5 920–8	0	1	3.9 4.3	1,560 2,440	0.71 1.25	0.37 0.48	(Choma et al. 2015)
PVDF	Ar 700–2 900–2	25	1	3.44 3.25	1,023 1,037	0.33 0.33	0.24 0.23	(Park et al., 2020)
PVDF	CO_2 800–2 900–2	25	1	3.73 3.31	1,154 1,158	0.38 0.37	0.26 0.24	(Park et al., 2020)
Kevlar	CO_2 750–3 850–1	7	15	6.5 10.3	469 1,109	–	0.19 0.22	(Conte et al., 2020)
PDF	CO_2 800–1	0 25 50	1	6.05 3.84 2.30	1,479	0.58	0.26	(Hong et al., 2016)
PDF	N_2 600–2 700–2	25	1	3.52 2.72	995 888	0.39 0.34	–	(Lee and Park, 2014)
PET	CO_2 925–24 925–72	25	4	4.85 6.59	984 2,176	0.25 0.29	–	(Moura et al., 2018)
Kevlar	CO_2 1000–0.25 1000–0.5	30	1	1.8 1.5	1,593 1,586	0.39 0.32	–	(Kaliszewski et al., 2021)
PS	Steam + gaseous ammonia 810–2	30	1	2.82 3.2	1,274 1,198	0.47 0.46	–	(Ren et al., 2022)

* Weight increase.

demonstrated that narrower micropores for CO_2 capture facilitate the retention of CO_2 in the pore walls. So, using high impregnation rates makes the micropores collapse, forming macropores, which are not favourable for CO_2 adsorption. A high degree of narrow porosity enables the full penetration of the CO_2 molecules into the pores: this seems to be a well- established fact in the adsorption performances of the activated carbons from different precursors (Hong et al., 2016; Rehman and Park, 2018a; Rehman and Park, 2018b).

Besides the pore characteristics, the nature of the interactions among the gas species and pore surface is also relevant for CO_2 adsorption. Some authors attempted to improve those interactions by doping nitrogen compounds into the carbon framework prior to the activation. Arenillas et al. (2005) studied the CO_2 capture capacity of a series of activated carbons obtained by mixing different nitrogen compounds (acridine, carbazole and urea) with PET wastes. The N-doped activated carbons showed a better capacity for CO_2 adsorption than the activated carbon prepared without nitrogen. Song et al. (2020) converted PET waste into N-doped carbon, using melamine and $ZnCl_2$/NaCl eutectic salts, and studied its adsorption capacity. The resulting material showed the adsorption capacity of 6.5 mmol g^{-1}, which was three times higher than the carbonized one. Yuan et al. (2020b) also produced N-doped carbon adsorbents from the same precursor by urea treatment and KOH activation. The samples activated with KOH and urea showed a higher CO_2 adsorption capacity than those without nitrogen dopants (6.23–5.30 mmol g^{-1}, respectively). The CO_2 molecule is largely quadrupolar and weakly acidic; thus, the introduction of basic nitrogen dopants onto the carbonaceous surface can boost the interaction between the acidic gas molecules and the surface of the pores (Kaur et al., 2019b). On the other hand, oxidation of the precursor prior to the activation is another feasible process for further enhancing the adsorption capacity toward acid gases. This approach includes blending of the precursor with the oxidizing species, followed by a heating step at moderate temperatures. The largest CO_2 uptakes of 8.93 and 6.9 mmol g^{-1} at ambient pressure were obtained for the pre-oxidized activated carbons (see Table 7). It should be noted that the oxidation of the surface increases the number of oxygen functional groups, opening the possibility of specific interactions between the CO_2 molecules and the oxygen groups.

The PAN waste-based activated carbons have also proved to be good CO_2 adsorbents. Singh et al. (2019c) produced PAN wastes at different activation temperatures, times and impregnation rates. The maximum CO_2 adsorption, 2.5 mmol g^{-1}, was obtained for the sample activated at 800 °C for 2 h at the KOH/precursor ratio of 3:1. This adsorption capacity was about 10 times greater than that of the untreated PAN (0.22 mmol g^{-1}). The sample produced under these conditions exhibited also the largest specific surface S_{BET} and pore volume. The same authors (Singh et al., 2019d) used other activating agents to prepare adsorbents from the same precursor. The activation was performed using $NaNH_2$, NaOH, and K_2CO_3. It was reported that the K_2CO_3-activated carbons showed the maximum adsorption capacity, (2.44 mmol g^{-1}), followed by the NaOH (2.20 mmol g^{-1}) and $NaNH_2$ (1.75 mmol g^{-1}) activated carbons. The maximum adsorption capacities were correlated by the authors with the S_{BET} and pore volume, which were the major factors to improve the CO_2 adsorption capacity. Kamran et al. (2020) studied the CO_2 adsorption capacity of porous PAN waste, using several chemical agents. It appeared that the adsorption capacity decreased in the following order: NaOH > KOH > K_2CO_3 > KNO_3. Interestingly, NaOH-activated samples exhibited significantly smaller values of S_{BET} and

pore volume than the KOH-activated ones. Although large surface areas have been reported to be beneficial for enhancing the CO_2 adsorption process, there is no strict correlation between the CO_2 adsorption capacity and the increase of the surface area and pore volume. Actually, it is possible to obtain large values of surface area due to the pores that are unsuitable for CO_2 adsorption but suitable for N_2 adsorption. This is attributed to the difference in the molecular sizes between N_2 (364 pm) and CO_2 (330 pm). The activated carbons with large micropores can be more selective for the N_2 molecules rather than the smaller CO_2 ones. Thus, the surface selectivity of gases -notably N_2– other than CO_2 should be considered when using adsorbents for CO_2 capture.

Another point to consider is the adsorbate-adsorbent interactions derived from the short-range attractive and repulsive forces (Gregg and Sing, 1991). These interactions can be significantly strengthened if the adsorption occurs in the narrow micropores i.e., < 0.8 nm, which enable the overlapping of the potential fields from the neighbouring pores (Sing, 1995). A high adsorption potential induces stronger interactions between the linker and the guest molecules. This mechanism leads to the complete filling of the pores, rather than their surface coverage, which typically occurs in the larger size pores.

4.2. CO_2 adsorption capacity of physically activated carbons

As follows from the literature reports, effective CO_2 adsorbents derived from plastic wastes can also be produced via physical activation. However, such studies are not numerous. As shown in Table 7, the CO_2 adsorption capacities for the physically activated carbons ranged from 6.5 to 1.5 mmol g^{-1} (1 atm). Park et al. (2020) reported that efficient CO_2 adsorbents could be obtained from poly(vinylidenefluoride) by activation under CO_2 or argon atmosphere. The carbonization and activation were conducted simultaneously. The Ar- and CO_2-activated carbons showed significant adsorption capacities of 3.44 and 3.73 mmol g^{-1} at 25 °C and 1 atm, respectively. The adsorption correlated with the narrow micropores volume, but not with the surface area and the total pore volume. Hong et al. (2016) prepared activated carbons from the same precursor by single-step physical activation and evaluated their CO_2 adsorption capacity. The activation was conducted in a CO_2 medium, at temperatures from 700 to 950 °C. The surface area and the total pore volume increased with the increasing activation temperature. However, the maximum adsorption capacity of 6.05 mmol g^{-1} was obtained for the sample activated at 800 °C. The authors concluded that the adsorption capacity was mainly dependent on the volume of micropores that were below 0.70 nm in size.

Some authors compared the adsorption performance of chemically and physically activated carbons. Ge et al. (2019) used polyurethane waste to prepare a series of activated carbons by physical activation with CO_2 and chemical activation with hydroxides. The samples obtained by the chemical activation showed a larger CO_2 adsorption capacity than the physical ones. The CO_2 adsorption capacity of 5.85 mmol g^{-1} was reported for the KOH-sample compared to 3.37 mmol g^{-1} obtained for the CO_2-sample. This was attributed to the larger volume of micropores (<1 nm) induced by the chemical activation. Similarly, Choma et al. (2014) prepared activated carbons by KOH and CO_2 activations of DVDs and CDs wastes and compared their CO_2 adsorption capacities. Under the optimal conditions, the KOH-sample showed the adsorption capacity of 5.7 mmol g^{-1} and the CO_2-sample of 4.3 mmol g^{-1} at 0 °C and 1 atm. For both activated carbons, the largest CO_2 adsorption coincided with the highest values of textural parameters.

Another important variable having a significant influence on the CO_2 capture capacity of any adsorbent is the operating adsorption pressure. Moura et al. (2018) prepared a series of activated carbons from PET waste by physical activation and evaluated their adsorption capacity in the pressure range of 1–10 atm. The amount of adsorbed CO_2 increased with the increasing adsorption pressure from 2 to 11 mmol g^{-1}. Similar findings were reported by Conte et al. (2020), who examined the adsorption capacity of Kevlar-based activated carbon in the pressure range of 0–15 atm. The largest adsorption capacity of 10.3 mmol g^{-1} was reported at 7 °C and 15 atm. A higher pressure of adsorbate forces gas molecules to have more contact at the binding sites on the adsorbent pores and thus promotes the adsorption efficiency. The adsorption at atmospheric pressure is effective when the pore size is compatible with the molecular CO_2 size, i.e., when the adsorbent exhibits narrow porosity structures. However, at higher pressures the adsorption is also efficient on wider pores, which increases the adsorption densities (Table 7). Lee and Park (2014) studied the adsorption properties of carbonized poly(vinylidene fluoride) at different pressures. The results showed that at 100 kPa, the adsorption capacity was mainly governed by the micropore volume, while the ultramicropores (<0.65 nm) were more suitable for the CO_2 molecules at pressures of<30 kPa.

All in all, the information obtained from the literature shows that the low cost, ready availability and finely-tuneable pore structure, together with the better working conditions, makes plastic wastes very promising precursors to prepare efficient adsorbents. The most important factors to consider in the synthesis of effective plastic-based CO_2 adsorbents are as follows:

(a) Pores size and shape: Tailoring the activated carbon pore diameter to match the CO_2 kinetic diameter significantly improves the CO_2 adsorption capacity. At ambient conditions, narrow micropore structures contribute to CO_2 molecules adsorption by a pore filling mechanism. In contrast, carbons containing larger pore sizes (>1 nm) are not capable of capturing dense packs of CO_2 molecules. Additionally, narrow microporosity structures provide a high selectivity towards CO_2 molecules in a CO_2/N_2 gas mixture. Consequently, the development of narrow porosity structures (<0.8 nm) is the main criterion to produce a suitable plastic-based CO_2 adsorbent. The development of larger pores is also effective at higher adsorption pressures. This can be achieved by adjusting the experimental conditions, the main activating agent and temperature. Moreover, structural analyses are recommended to describe the adsorption process based on the size and shape of the pores.

(b) Activations: i) Chemical - The chemically activated carbons exhibited better adsorption capacities than the physical ones (Table 7). The higher efficiency can be assigned to the fact that the former allows better control of the pore structure than the latter. The impregnation of the precursor with a specific agent concentration allows the desired pore structure to be obtained. Since it is capable of producing narrow porosity structures, KOH is the preferred chemical agent used for plastic waste activation. A higher impregnation ratio than 4 is not recommended when using this agent as it results in pore blockage, minimizing the adsorption capacity and selectivity (Alhamed et al., 2015). Other agents that exhibited good adsorption performances are NaOH or K_2CO_3, which also produce micropores with narrow diameters using low impregnation rates (Table 7). ii) Physical - The literature shows that CO_2 is preferable to other agents for preparing plastic-based CO_2 adsorbents. This agent provides the carbon with abundant narrow micropores (Table 7). More reactive agents such as steam or O_2 induce faster reactions with the carbon species, causing the expansion of the pores, which results in a more random porous structure. Consequently, highly reactive agents are not recommended for the present purpose. Nevertheless, dilution of these agents with inert gases could enhance the control of the activation process and thus, the adsorption capacity of the activated material. A general trend is that the micropore volume is related to the physical activation temperature when it is below 900 °C; higher temperatures are not recommended, as they can result in a pore wall collapse, forming macropores. Finally, despite its higher energy consumption, the two-step method, e.g. pyrolysis and activation, is more frequently used to produce plastic-based CO_2 adsorbents. This is justified by the

better porosity characteristics that this method provides compared to the single-step one.

(c) Interactions between adsorbate and adsorbent: The surface chemical composition also plays an important role in controlling the CO_2 adsorption density. The incorporation of nitrogen dopants increases the basicity of the carbon surface, enabling specific interactions between the acid CO_2 molecules and the carbon pores. As a source of nitrogen groups, agents like NH_3 or amine are recommended owing to their affinity towards the CO_2 molecules. Additionally, the functionalization of the activated carbon surface is also recommended. The presence of oxygen-containing groups induces a negative charge in the carbon surface, strengthening the interactions with the acidic CO_2 molecules. The oxygen functionalities can be induced by the oxidation of the carbon; i.e. by means of pre- or post-synthesis oxidative treatments. These treatments also contribute to enhance the selectivity towards CO_2 molecules adsorption (Shafeeyan et al., 2010).

Summarizing, the CO_2 adsorption capacity of plastic-based chars mainly depends on the combined effect of micropore volume, the presence of functional groups, basicity of the surface and adsorption conditions. The combination of these factors offers a wide range of new possibilities for the synthesis of effective adsorbents, depending on their final application. For instance, plastic-based activated carbons with specific porosity characteristics can be attractive candidates for the separation of CO_2 and CH_4 in biogas upgrading applications.

5. Upgrading of biogas using activated carbons produced from residual materials

Biogas results from the anaerobic digestion of organic materials and is mainly composed of CH_4 and CO_2 (Bharathiraja et al., 2016). It represents a potential resource to produce bioenergy, using a wide range of raw materials coming from wastes generated in industry or daily life. The main application of biogas is to produce energy, either thermal (direct burning in boilers), electrical (internal combustion engines or gas turbines) or both (cogeneration). A further step towards the exploitation of biogas is to clean it and upgrade it to produce biomethane. This process extends its use to multiple applications, including vehicle fuel or direct injection into the natural gas grids. Thus, its usage promotes progress in the circular economy action plan, less dependence on fossil fuels, and the reduction of environmental pollution.

Biogas upgrading refers to a gas separation process involving the removal of the main undesirable component of biogas, CO_2, and other trace species such as H_2O, NH_3 or H_2S. Since CO_2 reduces the calorific value of biogas, its removal is one of the most important upgrading steps. Compared with other upgrading technologies, the pressure swing adsorption (PSA) technique is attracting much interest owing to its lower energy demand and lower emissions (Agarwal et al., 2010). PSA exploits the difference between methane and CO_2 in terms of the degree of attraction to the surface under pressure. Separation is based on both molecular size exclusion and adsorption affinity. Activated carbons are among the most common adsorbents used in PSA units (Surra et al., 2022). Although abundant research has been performed on CO_2 adsorption on different adsorbents prepared from solid wastes, studies on the adsorption process for biogas upgrading are scarce. This section provides a summary of the key studies on the use of activated carbons derived from wastes (mainly biomass) as adsorbents for biogas upgrading. Additionally, the possible use of plastic-based activated carbon for that purpose is discussed.

5.1. Application of char-based activated carbons for biogas upgrading

Álvarez-Gutiérrez et al. (2016) prepared two biomass-based activated carbons from cherry stones using physical activation with steam and carbon dioxide. The samples were subjected to biogas upgrading by means of dynamic breakthrough experiments with a simulated binary gas steam (50/50 vol%). The authors concluded that the CO_2-activated samples were the most effective in the adsorption–desorption cycles, reaching CO_2 adsorption capacities of approximately 2 and 5.14 mmol g^{-1} at 1 and 10 bar, respectively. The CH_4 purity reached (>95 %) was higher than that reached by a commercial adsorbent (85 %) in the same working conditions. The authors reported that the differences in the polar moment between the CO_2 and CH_4 molecules induced a preferential adsorption of CO_2 over CH_4. The authors also pointed out the importance of developing narrow micropores in the biomass-based carbons. Surra et al. (2022) prepared activated carbons from maize wastes by CO_2 physical activation, varying the activation time, and studied their performance in biogas upgrading. The longer activation produced carbons with a higher surface area and micropore volume, which were more suitable for biogas upgrading. Vivo-Vilches et al. (2017) prepared activated carbon from commercial pine wood pellets by means of physical activation with carbon dioxide; the authors evaluated its behaviour as a CO_2 adsorbent for biogas upgrading, and observed that the material could separate CH_4 and CO_2, obtaining pure CH_4 from the 60 % CO_2 and 40 % CH_4 mixture; they concluded that the activation induced a large micropore widening, which led to a great selectivity of CO_2 in all ranges of pressure tested. Gallucci et al. (2020) investigated the CO_2 adsorption capacity of silver hydrochar for the sawdust obtained by means of hydrothermal carbonization and subsequent KOH activation in a model biogas mixture (50/50 vol%). The best CO_2 adsorption capacity of 6.56 mmol g^{-1} (5 bar) was reached for the sample characterized by a S_{BET} of 881 m^2g^{-1} and 1 nm pore diameter. Seo et al. (2016) also demonstrated effective biogas upgrading using bamboo char prepared by pyrolysis at different temperatures. The bamboo carbonized at the highest temperature (900 °C) exhibited the largest CO_2 adsorption capacity (2.76 mmol g^{-1}) and allowed>90 % of CH_4 stream to be obtained from the 60 % CH_4 and 40 % CO_2 mixture. The authors stated that the higher the temperature, the smaller the carbon pores and the closer to the CH_4 molecular size (0.38 nm). Lourenco et al. (2019) prepared chitosan-based materials using different strategies and evaluated their applicability for biogas upgrading. The adsorbent prepared by drying in supercritical CO_2 and subjected to later pyrolysis exhibited a very high affinity for CO_2 and a very low affinity for CH_4, with the highest selectivity value (95 at 500 kPa) in the CO_2/CH_4 separation. The presence of high nitrogen content and 2 nm micropores on the carbon surface seemed to promote the CO_2 adsorption process. Vilella et al. (2017) synthesized activated carbons from babassu coconut by means of physical activation with carbon dioxide and examined their application in biogas upgrading. The prepared activated carbons proved to be a promising material for biogas upgrading, with a selectivity of 4.2 at 1 bar and a CO_2 adsorption capacity of 1.0 mmol g^{-1} at 3 bar. Durán et al. (2022) reported that efficient activated carbons can be obtained from pine sawdust to remove the CO_2 from biogas streams. On the other hand, Linville et al. (2017) studied the use of biomass-based activated carbons in an in-situ biogas upgrading process. The modified version of the in-situ CO_2 removal was applied during the anaerobic digestion of food waste with two types of walnut shell biochar on the bench scale in the batch operating mode. The biochar could remove 40–96 % of the CO_2 compared with the control digesters under mesophilic and thermophilic temperature conditions.

As shown above, waste materials are promising candidates to produce efficient adsorbents for biogas upgrading. These materials exhibited a similar or even better potential than marketed products (Mulu

Table 8
Physical constant of gases.

Gas	Kinetic Diameter (nm)	Quadrupolar moment (Å^3)	Polarity (Å^3)
CO_2	0.33	0.64	1.9
N_2	0.364	0.31	1.4
CH_4	0.38	0	2.6

et al., 2021). Considering the intrinsic characteristics of plastic-based activated carbons, their use for biogas upgrading deserves to be explored. One of the main prerequisites of any suitable adsorbent is its tuneable texturation, which is one the main properties of those materials. Moreover, another essential parameter to consider is the CO_2 selectivity. In the previous section, it was shown that narrow microporosity structures provide high selectivity towards CO_2 molecules in a CO_2/N_2 gas mixture. This structural characterization hinders the diffusion of N_2 molecules into the pores, which is attributed to the differences between the CO_2 and N_2 molecular sizes. The similar kinetic diameters of the CH_4 and N_2 molecules (Table 8) suggest that plastic-based adsorbents could also achieve a high selectivity for CO_2/CH_4 mixtures. In fact, some authors emphasise the importance of developing narrow micropore structures in biomass-based adsorbents (<0.8 nm) for biogas upgrading (Seo et al., 2016; Gallucci et al., 2020; Vivo-Vilches et al., 2017).

Furthermore, in any interpretation of the adsorption process, the fundamental properties of the adsorbate species must be considered. In physical adsorption, the interaction forces between the carbon surface and the guest molecule are a function of their polarity (Sing, 1995). For a CO_2/N_2 mixture, the adsorption is based on the higher quadrupolar moment of the CO_2 molecules (Table 8), which induces stronger pore wall interactions. The decrease in the polar moments in the sequence $CH_4 < N_2 < CO_2$ suggests that the CO_2 molecules would be adsorbed preferentially, leading to the purification of a CH_4/CO_2 gas mixture. Based on these premises, plastic-based activated carbons should have the potential to be applied effectively for selective adsorption of CO_2 over CH_4. Nevertheless, it is challenging to remove CO_2 to a high degree from a gas mixture, only tailoring the porosity of the adsorbent. Since the CO_2 adsorption capacity significantly decreases at elevated temperatures, additional treatments that strengthen the interactions between CO_2 and the adsorbent surface should be considered. The functionalization of the carbon surface, e.g. by means of introducing of oxygen- or nitrogen-containing groups, along with the appropriate activation, could play a combined role for achieving higher CO_2 adsorption and better selectivity performance. In this way, the applicability of plastic-based adsorbents for that purpose seems to be very feasible.

6. Conclusions; challenges and avenues for future research

Plastic management is a hot topic that needs to be addressed very seriously. In this regard, the search for new applications of plastic waste materials is crucial. An unexplored area includes the development of plastic-based activated carbons for the adsorption of CO_2 in biogas upgrading. The most important parameters to produce activated carbon for CO_2 capture are the following: the composition and chemical structure of the raw precursor material; the selection of a suitable activating agent; the time and temperature of pyrolysis and activation. The chemical activation of carbons provides better control of the development of porosity than the physical one, resulting in better adsorption capacities. However, physical activation is simpler, cheaper, and more favourable in terms of environmental safety. The main governing mechanism in the adsorption process is the development of narrow porous structures, especially at atmospheric pressure. The reasons for exploring the applicability of plastic-based activated carbons for biogas upgrading lies in their tuneability, high surface area, large micropore volume, availability of precursors, thermal stability, high degree of CO_2 adsorption and the high selectivity towards CO_2 over CH_4 based on the molecular size exclusion and electric field gradient.

Although progress has been made in plastic-based adsorbent materials via pyrolysis, there are still some challenges to face before these adsorbents can be used in large-scale industrial settings. One of these is the need to verify the desorption of CO_2 and adsorbent regeneration to achieve the application of biogas upgrading on a large scale. The goal is to recycle the adsorbent as many times as possible before its final disposal, aiming to make it cost-effective. In addition to the high adsorption capacity and long-term recyclability, its stability and resistance have yet to be comprehensively determined. Another important challenge is environmental risk assessment, alongside economic and environmental feasibility analyses. Since chemical activation implies the use of agents such as KOH, H_3PO_4 or $ZnCl_2$ that may have a negative environmental impact, the development of more environmentally friendly alternatives can and must be an important research direction. Another important challenge involves the in-depth investigation of CO_2 removal mechanisms. In general, mechanistic aspects of how to improve functionalization are less often addressed. Further studies should in any case include helpful information about the intrinsic mechanisms of CO_2 capture to develop more targeted plastic-based char activation/modification schemes. The activated carbon adsorption rate tends to drop when operated at high temperature as well as low pressure conditions. Thus, testing and optimization of these materials in order to withstand these environments and attain a high CO_2 adsorption density is needed. Another of the major challenges for the pyrolysis of plastic wastes is the still non-existent markets for the solid product (char) and unclear regulations concerning plastic waste management. Post-consumer plastic wastes that are not collected separately may contain pigments, metal foils, coatings, etc., that affect the quality of the char, and consequently, its by-products. Lastly, simulated gases were employed in most of the biogas upgrading studies reported; thus, real-world biogas effluents (composition and circumstances) must be examined. The existence of other pollutants can reduce the adsorbents' durability and efficiency, resulting in higher operating costs.

All in all, more research is required on the preparation and applications of plastic-based activated carbons from the perspective of their industrial applicability. Environmental and economic studies, regeneration research and evaluation of these materials in real industrial environments are required. The use of plastic waste adsorbents for biogas upgrading seems to be a promising and feasible possibility. Therefore, further research on this topic is highly recommended.

Declaration of Competing Interest

The authors declare that they have no known competing financial interests or personal relationships that could have appeared to influence the work reported in this paper.

Data availability

No data was used for the research described in the article.

Acknowledgements

This paper has received funds from the project PID2019.108826RB. I00 financied by MCIN/ AEI /10.13039/501100011033. Funding for open access charge: Universidad de Granada / CBUA. Our gratitute to Prof. Fernando González-Caballero for his support and fruitful comments during the preparation of the manuscript.

References

Adibfar, M., Kaghazchi, T., Asasian, N., Soleimani, M., 2014. Conversion of poly (ethylene terephthalate) waste into activated carbon: chemical activation and characterization. Chem. Eng. Technol. 37 (6), 979–986. https://doi.org/10.1002/ceat.201200719.

Adrados, A., de Marco, I., Caballero, B.M., López, A., Laresgoiti, M.F., Torres, A., 2012. Pyrolysis of plastic packaging waste: A comparison of plastic residuals from material recovery facilities with simulated plastic waste. Waste Manag. 32 (5), 826–832. https://doi.org/10.1016/j.wasman.2011.06.016.

Agarwal, A., Biegler, L.T., Zitney, S.E., 2010. A super structure-based optimal synthesis of PSA cycles for post-combustion CO_2 capture. AIChE J. 56, 1813–1828. https://doi.org/10.1002/aic.12107.

Ahangar, F.A., Rashid, U., Ahmad, J., Tsubota, T., Alsalme, A., 2021. Conversion of Waste Polyethylene Terephthalate (PET) Polymer into Activated Carbon and Its

Feasibility to Produce Green Fuel. Polymers 13 (22), 3952. https://doi.org/10.3390/polym13223952.
Ahmed, S.F., Mofijur, M., Tarannum, K., Chowdhur, A.T., Rafa, N., Nuzhat, S., Kumar, P. S., Vo, D.-V.-N., Lichtfouse, E., Mahlia, T.M.I., 2021. Biogas upgrading, economy and utilization: a review. Environ. Chem. Lett. 19 (6), 4137–4164. https://doi.org/10.1007/s10311-021-01292-x.
Akmil-Başar, C., Önal, Y., Kılıçer, T., Eren, D., 2005. Adsorptions of high concentration malachite green by two activated carbons having different porous structures. J. Hazard. Mater. 127 (1–3), 73–80. https://doi.org/10.1016/j.jhazmat.2005.06.025.
Alhamed, Y.A., Rather, S.U., El-Shazly, A.H., Zaman, S.F., Daous, M.A., Al-Zahrani, A.A., 2015. Preparation of activated carbon from fly ash and its application for CO_2 capture. Korean J. Chem. Eng. 32, 723–730. https://doi.org/10.1007/s11814-014-0273-2.
Al-Salem, S.M., Antelava, A., Constantinou, A., Manos, G., Dutta, A., 2017. A review on thermal and catalytic pyrolysis of plastic solid waste (PSW). J. Environ. Manage. 197, 177–198. https://doi.org/10.1016/j.jenvman.2017.03.084.
Almazán-Almazán, M.C., Pérez-Mendoza, M., Domingo-García, M., Fernández-Morales, I., López, F.J., López-Garzón, F.J., 2010. The influence of the process conditions on the characteristics of activated carbons obtained from PET de-polymerisation. Fuel Process. Technol. 91 (2), 236–242. https://doi.org/10.1016/j.fuproc.2009.10.003.
Almazán-Almazán, M.C., Pérez-Mendoza, M., López-Domingo, F.J., Fernández-Morales, I., Domingo-García, M., López-Garzón, F.J., 2007. A new method to obtain microporous carbons from PET: Characterisation by adsorption and molecular simulation. Micropor. Mesopor. Mat. 106 (1–3), 219–228. https://doi.org/10.1016/j.micromeso.2007.02.053.
Almroth, B.C., Eggert, H., 2019. Marine Plastic Pollution: Sources, Impacts, and Policy Issues. Rev. Env. Econ. Policy 13 (2), 317–326. https://doi.org/10.1093/reep/rez012.
Álvarez-Gutiérrez, N., García, S., Gil, M.V., Rubiera, F., Pevida, C., 2016. Dynamic performance of biomass-based carbons for CO_2/CH_4 separation. Approximation to a pressure swing adsorption process for biogas upgrading. Energy Fuels 30 (6), 5005–5015. https://doi.org/10.1021/acs.energyfuels.6b00664.
Álvarez-Gutiérrez, N., Gil, M.V., Rubiera, F., Pevida, C., 2018. Simplistic approach for preliminary screening of potential carbon adsorbents for CO_2 separation from biogas. J. CO_2 Util. 28, 207–215. https://doi.org/10.1016/j.jcou.2018.10.001.
Arami-Niya, A., Daud, W.M.A.W., Mjalli, F.S., 2010. Using granular acti- vated carbon prepared from oil palm shell by $ZnCl_2$ and physical activation for methane adsorption. J. Anal. Appl. Pyrol. 89 (2), 197–203. https://doi.org/10.1016/j.jaap.2010.08.006.
Arenillas, A., Rubiera, F., Parra, J.B., Ania, C.O., Pis, J.J., 2005. Surface modification of low cost carbons for their application in the environmental protection. Appl. Surf. Sci. 252 (3), 619–624. https://doi.org/10.1016/j.apsusc.2005.02.076.
Attia, A.A., Girgis, B.S., Fathy, N.A., 2008. Removal of methylene blue by carbons derived from peach stones by H3PO4 activation: batch and column studies. Dyes Pigm. 76 (1), 282–289. https://doi.org/10.1016/j.dyepig.2006.08.039.
Bai, B.C., Kim, E.A., Lee, C.W., Lee, Y.-S., 2015. Effects of surface chemical properties of activated carbon fibers modified by liquid oxidation for CO2 adsorption. Appl. Surf. Sci. 353, 158–164. https://doi.org/10.1016/j.apsusc.2015.06.046.
Bailar, J.C., Trotaman-Dickenson, A.F. (Eds.), 1973. Comprehensive Inorganic Chemistry, vol. I. Pergamon Press, Oxford.
Balat, M., Balat, M., Kirtay, E., Balat, H., 2009. Main routes for the thermo-conversion of biomass into fuels and chemicals. Part 1: Pyrolysis systems. Energy Conv. Manag. 50, 3147–3157. https://doi.org/10.1016/j.enconman.2009.08.014.
Balsamo, M., Budinova, T., Erto, A., Lancia, A., Petrova, B., Petrov, N., Tsyntsarski, B., 2013. CO_2 adsorption onto synthetic activated carbon: Kinetic, thermodynamic and regeneration studies. Sep. Purif. Technol. 116, 214–221. https://doi.org/10.1016/j.seppur.2013.05.041.
Belo, C.R., Cansado, I.P.P., Mourão, P.A.M., 2017. Synthetic polymers blend used in the production of highactivated carbon for pesticides removals from liquid phase. Environ. Technol. 38 (3), 285–296. https://doi.org/10.1080/09593330.2016.1190409.
Bhatnagar, A., Hogland, W., Marques, M., Sillanpää, M., 2013. An overview of the modification methods of activated carbon for its water treatment applications. Chem. Eng. J. 219, 499–511. https://doi.org/10.1016/j.cej.2012.12.038.
Benadjemia, M., Millière, L., Reinert, L., Benderdouche, N., Duclaux, L., 2011. Preparation, characterization and Methylene Blue adsorption of phosphoric acid activated carbons from globe artichoke leaves. Fuel Process. Technol. 92 (6), 1203–1212. https://doi.org/10.1016/j.fuproc.2011.01.014.
Benedetti, V., Patuzzi, F., Baratieri, M., 2017. Gasification char as a potential substitute of activated carbon in adsorption applications. Energy Procedia 105, 712–717. https://doi.org/10.1016/j.egypro.2017.03.380.
Bharathiraja, B., Sudharsanaa, T., Bharghavi, A., Jayamuthunagai, J., Praveenkumar, R., 2016. Biohydrogen and Biogas – An overview on feedstocks and enhancement process. Fuel 185, 810–828. https://doi.org/10.1016/j.fuel.2016.08.030.
Bishop, G., Styles, D., Lens, P., 2020. Recycling of European plastic is a pathway for plastic debris in the ocean. Environ. Int. 142, 105893 https://doi.org/10.1016/j.envint.2020.105893.
Bóta, A., László, K., Nagy, L.G., Copitzky, T., 1997. Comparative study of active carbons from different precursors. Langmuir 13 (24), 6502–6509. https://doi.org/10.1021/la9700883.
Bratek, W., Świątkowski, A., Pakuła, M., Biniak, S., Bystrzejewski, M., Szmigielski, R., 2013. Characteristics of activated carbon prepared from waste PET by carbon dioxide activation. J. Anal. Appl. Pyrol. 100, 192–198. https://doi.org/10.1016/j.jaap.2012.12.021.
Butler, K.M.E., Devlin, G., 2011. Waste polyolefins to liquid fuels via pyrolysis: review of commercial state-of-the-art and recent laboratory research. Waste Biomass Valor. (2), 227–255. https://doi.org/10.1007/s12649-011-9067-5.
Cansado, I.P.P., Ribeiro Carrott, M.M.L., Carrott, P.J.M., Mourão, P.A.M., 2008. Textural development of activated carbon prepared from recycled PET with different chemical activation agents. Mater. Sci. Forum (587), 753–757. https://doi.org/10.4028/www.scientific.net/MSF.587-588.753.
Cansado, I.P.P., Galacho, C., Nunes, A.S., Carrott, M.L.R., Carrott, P.J.M., 2010. Adsorption properties of activated carbons prepared from recycled PET in the removal of organic pollutants from aqueous solutions. Adsorpt. Sci. Technol. 28 (8–9), 807–821. https://doi.org/10.1260/0263-6174.28.8-9.807.
Cansado, I.P.P., Mourão, P.A.M., Nabais, J.M.V., Tita, B., Batista, T., Rocha, T., Borges, C., Matos, G., 2022. Use of dirty plastic wastes as precursors for activated carbon production – a contribution to the circular economy. Water Environ. J. 36 (1), 96–104. https://doi.org/10.1111/wej.12762.
Calvino-Casilda, V., López-Peinado, A.J., Durán-Valle, C.J., Martín-Aranda, R.M., 2010. Last decade of research on activated carbons as catalytic support in chemical processes. Catal. Rev. 52 (3), 325–380. https://doi.org/10.1080/01614940.2010.498748.
Cetin, E., Moghtaderi, B., Gupta, R., Wall, T.F., 2004. Influence of pyrolysis conditions on the structure and gasification reactivity of biomass chars. Fuel 83, 2139–2150. https://doi.org/10.1016/j.fuel.2004.05.008.
Chen, C., Wang, J., Liu, W., Zhang, S., Yin, J., Luo, G., Yao, H., 2013. Effect of pyrolysis conditions on the char gasification with mixtures of CO2 and H2O. Proc. Combust. Inst. 34 (2), 2453–2460. https://doi.org/10.1016/j.proci.2012.07.068.
Chen, S., Liu, Z., Jiang, S., Hou, H., 2020. Carbonization: A feasible route for reutilization of plastic wastes. Sci. Total Environ. 710, 136250 https://doi.org/10.1016/j.scitotenv.2019.136250.
Cheng, C., Liu, H., Dai, P., Shen, X., Zhang, J., Zhao, T., Zhu, Z., 2016. Microwave-assisted prepara- tion and characterization of mesoporous activated carbon from mushroom roots by phytic acid ($C_6H_{18}O_{24}P_6$) activation. J. Taiwan Inst. Chem. Eng. 67, 532–537. https://doi.org/10.1016/j.jtice.2016.08.032.
Chiang, Y.C., Yeh, C.Y., Weng, C.H., 2019. Carbon dioxide adsorption on porous and functionalized activated carbon fibers. Appl. Sci. 9 (10), 1977. https://doi.org/10.3390/app9101977.
Choma, J., Osuchowski, L., Dziura, A., Kwiatkowska-Wójcik, W., Mietek, J., 2014. Adsorption Properties of Active Carbons Obtained from Kevlar (R) Fibers. Ochr. Sr. 36 (4), 3–8.
Choma, J., Marszewski, M., Osuchowski, L., Jagiello, J., Dziura, A., Jaroniec, M., 2015. Adsorption Properties of Activated Carbons Prepared from Waste CDs and DVDs. ACS Sustain. Chem. Eng. 3 (4), 733–742. https://doi.org/10.1021/acssuschemeng.5b00036.
Choma, J., Osuchowski, L., Marszewski, M., Dziura, A., Jaroniec, M., 2016. Developing microporosity in Kevlar®-derived carbon fibers by CO2 activation for CO2 adsorption. J. CO2 Util. 16, 17–22. https://doi.org/10.1016/j.jcou.2016.05.004.
Collin, G.J., Anisuzzaman, S.M., Moh, P.Y., Lim, E.-W.-A., 2016. Sorption and Characterization Studies of Activated Carbon Prepared from Polyethylene Terephthalate (PET). Borneo science 37 (2), 28–39.
Conte, G., Stelitano, S., Policicchio, A., Minuto, F.D., Lazzaroli, V., Galiano, F., Agostino, R.G., 2020. Assessment of activated carbon fibers from commercial Kevlar® as nanostructured material for gas storage: Effect of activation procedure and adsorption of CO_2 and CH_4. J. Anal. Appl. Pyrol. 152, 104974 https://doi.org/10.1016/j.jaap.2020.104974.
Cui, X., Jia, F., Chen, Y., Gan, J., 2011. Influence of single-walled carbon nanotubes on microbial availability of phenanthrene in sediment. Ecotoxicology 20, 1277–1285. https://doi.org/10.1007/s10646-011-0684-3.
Czepirski, L., Szczurowski, J., Bałys, M., Ciesińska, W., Makomaski, G., Zieliński, G.J., 2013. Pore structure of activated carbons from waste polymers. Inż. Och. Śr. 16 (3), 353–359.
Djahed, B., Shahsavani, E., Naji, F.K., Mahvi, A.H., 2015. A novel and inexpensive method for producing activated carbon from waste polyethylene terephthalate bottles and using it to remove methylene blue dye from aqueous solution. Desalin. Water Treat. 57 (21), 9871–9880. https://doi.org/10.1080/19443994.2015.1033647.
de Castro, C.S., Viau, L.N., Andrade, J.T., Mendonça, T.A.P., Gonçalves, M., 2018. Mesoporous activated carbon from polyethyleneterephthalate (PET) waste: pollutant adsorption in aqueous solution. New J. Chem. 42, 14612–14619. https://doi.org/10.1039/C8NJ02715C.
de Paula, F.G.F., de Castro, M.C.M., Ortega, F.P.R., Blanco, C., Lavall, R.L., Santamaría, R., 2018. High value activated carbons from waste polystyrene foams. Microporous Mesoporous Mat. 267, 181–184. https://doi.org/10.1016/j.micromeso.2018.03.027.
Demirbas, A., 2004. Pyrolysis of municipal plastic wastes for recovery of gasoline-range hydrocarbons. J. Anal. Appl. Pyrol. 72 (1), 97–102. https://doi.org/10.1016/j.jaap.2004.03.001.
Domínguez-Ramos, L., Prieto-Estalrich, A., Malucelli, G., Gómez-Díaz, D., Freire, M.S., Lazzari, M., González-Álvarez, J., 2022. N- and S-Doped Carbons Derived from Polyacrylonitrile for Gases Separation. Sustainability 14, 3760. https://doi.org/10.3390/su14073760.
Elordi, G., Olazar, M., López, G., Artetxe, M., Bilbao, J., 2011. Product Yields and Compositions in the Continuous Pyrolysis of High-Density Polyethylene in a Conical Spouted Bed Reactor. Ind. Eng. Chem. Res. 50 (11), 6650–6659. https://doi.org/10.1021/ie200186m.
Esfandiari, A., Tahereh, K., Mansooreh, S., 2011. Preparation of high surface area activated carbon from polyethyleneterephthalate (PET) waste by physical activation. Res. J. Chem. Environ 15 (2), 433–437.

Esfandiari, A., Kaghazchi, T., Soleimani, M., 2012. Preparation and evaluation of activated carbons obtained by physical activation of polyethyleneterephthalate (PET) wastes. J. Taiwan Inst. Chem. Eng. 43 (4), 631–637. https://doi.org/10.1016/j.jtice.2012.02.002.

FakhrHoseini, S.M., Dastanian, M., 2013. Predicting Pyrolysis Products of PE, PP, and PET Using NRTL Activity Coefficient Model. J. Chem. 2013, 1–5. https://doi.org/10.1155/2013/487676.

Feng, B., Shen, W., Shi, L., Qu, S., 2018. Adsorption of hexavalent chromium by polyacrylonitrile-based porous carbon from aqueous solution. R. Soc. Open Sci. 5 (1), 171662 https://doi.org/10.1098/rsos.171662.

Fernández-Morales, I., Almazán-Almazán, M.C., Pérez-Mendoza, M., Domingo-García, M., López-Garzón, F.J., 2005. PET as precursor of microporous carbons: preparation and characterization. Micropor. Mesopor. Mater. 80 (1–3), 107–115. https://doi.org/10.1016/j.micromeso.2004.12.006.

Ford, H.V., Jones, N.H., Davies, A.J., Godley, B.J., Jambeck, J.R., Napper, I.E., Suckling, C.C., Williams, G.J., Woodall, L.C., Koldewey, H.J., 2022. The fundamental links between climate change and marine plastic pollution. Sci. Total Environ. 806, 150392 https://doi.org/10.1016/j.scitotenv.2021.150392.

Gallucci, K., Taglieri, L., Papa, A.A., Di Lauro, F., Ahmad, Z., Gallifuoco, Z.A., 2020. Non-energy valorization of residual biomasses via HTC: CO_2 capture onto activated hydrochars. Appl. Sci. 10 (5), 1879. https://doi.org/10.3390/app10051879.

Ge, C., Song, J., Qin, Z., Wang, J., Fan, W., 2016. Polyurethane Foam-Based Ultramicroporous Carbons for CO_2 Capture. ACS Appl. Mater. Interfaces 8 (29), 18849–18859. https://doi.org/10.1021/acsami.6b04771.

Ge, C., Lian, D., Cui, S., Gao, J., Lu, J., 2019. Highly Selective CO2 Capture on Waste Polyurethane Foam-Based Activated Carbon. Processes 7 (9), 592. https://doi.org/10.3390/pr7090592.

Gholipour, F., Mofarahi, M., 2016. Adsorption equilibrium of methane and carbon dioxide on zeolite13X: Experimental and thermodynamic modelling. J. Supercrit. Fluids 111, 47–54. https://doi.org/10.1016/j.supflu.2016.01.008.

Giraldo, L., Ladino, Y., Pirajánc, J.C.M., Rodríguez, M.P., 2007. Synthesis and characterization of activated carbon fibres from Kevlar. Eclet. Quim. 32 (4), 55–62. https://doi.org/10.1590/S0100-46702007000400008.

Golmakani, A., Nabavi, S.A., Wadi, B., Manovic, V., 2022. Advances, challenges, and perspectives of biogas cleaning, upgrading, and utilisation. Fuel 317, 123085. https://doi.org/10.1016/j.fuel.2021.123085.

Gómez-Serrano, V., Adame-Pereira, M., Alexandre-Franco, M., Fernández-González, C., 2021. Adsorption of bisphenol A by activated carbon developed from PET waste by KOH activation. Environ. Sci. Pollut. Res. 28 (19), 24342–24354. https://doi.org/10.1007/s11356-020-08428-6.

Gong, J., Michalkiewicz, B., Chen, X., Mijowska, E., Liu, J., Jiang, Z., Wen, X., Tang, T., 2014. Sustainable conversion of mixed plastics into porous carbon nanosheets with high performances in uptake of carbon dioxide and storage of hydrogen. ACS Sustain. Chem. Eng. 2 (12), 2837–2844. https://doi.org/10.1021/sc500603h.

González, J.F., Encinar, J.M., González-García, C.M., Sabio, E., Ramiro, A., Canito, J.L., Gañán, J., 2006. Preparation of activated carbons from used tyres by gasification with steam and carbon dioxide. Appl. Surf. Sci. 252 (17), 5999–6004. https://doi.org/10.1016/j.apsusc.2005.11.029.

Gregg, S.J., Sing, K.S.W., 1991. In Adsorption, surface area and porosity. Academic Press, London.

Guddeti, R.R., Knight, R., Grossmann, E.D., 2000. Depolymerization of polypropylene in an induction-coupled plasma (ICP) reactor. Ind. Eng. Chem. Res. 39 (5), 1171–1176. https://doi.org/10.1021/ie9906868.

Guizani, C., Jeguirim, M., Gadiou, R., Escudero Sanz, F.J., Salvador, S., 2016. Biomass char gasification by H2O, CO2 and their mixture: Evolution of chemical, textural and structural properties of the chars. Energy 112, 133–145. https://doi.org/10.1016/j.energy.2016.06.065.

Gunawardene, O.H.P., Gunathilake, C.A., Vikrant, K., Amaraweera, S.M., 2022. Carbon dioxide capture through physical and chemical adsorption using porous carbon materials: A review. Atmos. 13 (3), 397. https://doi.org/10.3390/atmos13030397.

Hadi, P., Yeung, K.Y., Guo, J., Wang, H., McKay, G., 2016. Sustainable development of tyre char-based activated carbons with different textural properties for value-added applications. J. Environ. Manage. 170, 1–7. https://doi.org/10.1016/j.jenvman.2016.01.005.

Hayashi, J., Yamamoto, N., Horikawa, T., Muroyama, K., Gomes, V.G., 2005. Preparation and characterization of high-specific-surface-area activated carbons from K2CO3-treated waste polyurethane. J. Colloid Interf. Sci. 281 (2), 437–443. https://doi.org/10.1016/j.jcis.2004.08.092.

Hock, P.E., Zaini, M.A.A., 2018. Activated carbon by zinc chloride activation for dye removal – a commentary. Acta Chim. Slov. 11 (2), 99–106. https://doi.org/10.2478/acs-2018-0015.

Hong, S.M., Choi, S.W., Kim, S.H., Lee, K.B., 2016. Porous carbon based on polyvinylidene fluoride: Enhancement of CO2 adsorption by physical activation. Carbon 99, 354–360. https://doi.org/10.1016/j.carbon.2015.12.012.

Hsiao, H.Y., Hung, C.-H., Hsu, M.Y., Chen, H., 2011. Preparation of high-surface-area PAN-based activated carbon by solution-blowing process for CO2 adsorption. Sep. Purif. Technol. 82, 19–27. https://doi.org/10.1016/j.seppur.2011.08.006.

Huang, Y.P., Hou, C.H., His, H.C., Wu, J.W., 2015. Optimization of highly microporous activated carbon preparation from Moso bamboo using central composite design approach. J. Taiwan Inst. Chem. Eng. 50, 266–275. https://doi.org/10.1016/j.jtice.2014.12.019.

Illán-Gómez, M.J., García-García, A., Salinas-Martínez de Lecea, C., Linares-Solano, A., 1996. Activated carbons from Spanish coals. 2. Chemical activation. Energy Fuels 10 (5), 1108–1114. https://doi.org/10.1021/ef950195%2B.

Ioannidou, O., Zabaniotou, A., 2007. Agricultural residues as precursors for activated carbon production—A review. Renew. Sust. Energ. Rev. 11 (9), 1966–2005. https://doi.org/10.1016/j.rser.2006.03.013.

Jagtoyen, M., Derbyshire, F., 1998. Activated carbons from yellow poplar and white oak by H_3PO_4 activation. Carbon 36 (7–8), 1085–1097. https://doi.org/10.1016/S0008-6223(98)00082-7.

Jahirul, M., Rasul, M., Chowdhury, A., Ashwath, N., 2012. Biofuels Production through Biomass Pyrolysis — A Technological Review. Energies 5 (12), 4952–5001. https://doi.org/10.3390/en5124952.

Jamradloedluk, J., Lertsatitthanakorn, C., 2014. Characterization and Utilization of Char Derived from Fast Pyrolysis of Plastic Wastes. Procedia Eng. 69, 1437–1442. https://doi.org/10.1016/j.proeng.2014.03.139.

Johnson, O., Joseph, B., Kuhn, J.N., 2021. CO_2 separation from biogas using PEI-modified crosslinked polymethacrylate resin sorbent. J. Ind. Eng. Chem. 103, 256–263. https://doi.org/10.1016/j.jiec.2021.07.038.

Jung, S.H., Cho, M.H., Kang, B.S., Kim, J.S., 2010. Pyrolysis of a fraction of waste polypropylene and polyethylene for the recovery of BTX aromatics using a fluidized bed reactor. Fuel Process. Technol. 91 (3), 277–284. https://doi.org/10.1016/j.fuproc.2009.10.009.

Kadirova, Z., Kameshima, Y., Nakajima, A., Okada, K., 2006. Preparation and sorption properties of porous materials from refuse paper and plastic fuel (RPF). J. Hazard. Mater. 137 (1), 352–358. https://doi.org/10.1016/j.jhazmat.2006.02.008.

Kakuta, N., Shimizu, A., Ohkita, H., Mizushima, T., 2009. Dehydrochlorination behavior of polyvinyl chloride and utilization of carbon residue: effect of plasticizer and inorganic filler. J. Mater. Cycles Waste Manag. 11 (1), 23–26. https://doi.org/10.1007/s10163-008-0214-4.

Kaliszewski, M., Zgrzebnicki, M., Kałamaga, A., Pinjara, S., Wróbel, R.J., 2021. Commercial Kevlar derived activated carbons for CO_2 and C_2H_4 sorption. Pol. J. Chem. Technol. 23 (2), 81–87. https://doi.org/10.2478/pjct-2021-0021.

Kamran, U., Choi, J.R., Park, S.-J., 2020. A Role of Activators for Efficient CO_2 Affinity on Polyacrylonitrile-Based Porous Carbon Materials. Front. Chem. 8, 710. https://doi.org/10.3389/fchem.2020.00710.

Kang, B.S., Kim, S.G., Kim, J.S., 2008. Thermal degradation of poly(methyl methacrylate) polymers: Kinetics and recovery of monomers using a fluidized bed reactor. J. Anal. Appl. Pyrol. 81 (1), 7–13. https://doi.org/10.1016/j.jaap.2007.07.001.

Kang, S., Jiang, S., Peng, Z., Lu, Y., Guo, J., Li, J., Zeng, W., Lin, X., 2018. Valorization of humins by phosphoric acid activation for activated carbon production. Biomass Convers. Biorefinery 8 (4), 889–897. https://doi.org/10.1007/s13399-018-0329-3.

Kartel, N.T., Gerasimenko, N.V., Tsyba, N.N., Nikolaichuk, A.D., Kovtun, G.A., 2001. Synthesis and Study of Carbon Sorbent Prepared from Polyethylene Terephthalate. Russ. J. Appl. Chem. 74 (10), 1765–1767. https://doi.org/10.1023/A:1014894211046.

Kartel, M.T., Sych, N.V., Tsyba, M.M., Strelko, V.V., 2006. Preparation of porous carbons by chemical activation of polyethyleneterephthalate. Carbon 44 (5), 1019–1022. https://doi.org/10.1016/j.carbon.2005.10.031.

Kaur, B., Gupta, R.K., Bhunia, H., 2019a. Chemically activated nanoporous carbon adsorbents from waste plastic for CO_2 capture: Breakthrough adsorption study. Microporous Mesoporous Mat. 282, 146–158. https://doi.org/10.1016/j.micromeso.2019.03.025.

Kaur, B., Singh, J., Gupta, R.K., Bhunia, H., 2019b. Porous carbons derived from polyethylene terephthalate (PET) waste for CO_2 capture studies. J. Environ. Manage. 242, 68–80. https://doi.org/10.1016/j.jenvman.2019.04.077.

Khamkeaw, A., Jongsomjit, B., Robison, J., Phisalaphong, M., 2019. Activated carbon from bacterial cellulose as an effective adsorbent for removing dye from aqueous solution. Sep. Sci. Technol. 54 (14), 2180–2193. https://doi.org/10.1080/01496395.2018.1541906.

Khan, M.U., Lee, J.T.E., Bashir, M.A., Dissanayake, P.D., Ok, Y.S., Tong, Y.W., Shariati, M.A., Wu, S., Ahring, B.K., 2021. Current status of biogas upgrading for direct biomethane use: A review. Renew. Sust. Energ. Rev. 149, 111343 https://doi.org/10.1016/j.rser.2021.111343.

Kim, Y.K., Kim, G.M., Lee, J.W., 2015. Highly porous N-doped carbons impregnated with sodium for efficient CO_2 capture. J. Mater. Chem. A 3 (20), 10919–10927. https://doi.org/10.1039/C5TA01776A.

Kong, L.B., Que, W., Liu, L., Boey, F.Y.C., Xu, Z.J., Zhou, K., Wang, C., 2017. Carbon Based Supercapacitors, Nanomaterials for Supercapacitors. CRC Press.

Kumar, U., Gaikwad, V., Mayyas, M., Sahajwalla, V., Joshi, R.K., 2018. Extraordinary supercapacitance in activated carbon produced via a sustainable approach. J. Power Sources 394, 140–147. https://doi.org/10.1016/j.jpowsour.2018.05.054.

Lam, S.S., Chase, H.A., 2012. A Review on Waste to Energy Processes Using Microwave Pyrolysis. Energies 5, 4209–4232. https://doi.org/10.3390/en5104209.

László, K., Bóta, A., Nagy, L.G., 2000. Comparative adsorption study on carbons from polymer precursors. Carbon 38 (14), 1965–1976. https://doi.org/10.1016/S0008-6223(00)00038-5.

Laszlo, K., Szucs, A., 2001. Surface characterization of polyethyleneterephthalate (PET) based activated carbon and the effect of pH on its adsorption capacity from aqueous phenol and 2,3,4-trichlorophenol solutions. Carbon 39 (13), 1945–1953. https://doi.org/10.1016/S0008-6223(01)00005-7.

László, K., 2005. Adsorption from aqueous phenol and aniline solutions on activated carbons with different surface chemistry. Colloid Surf. A-Physicochem. Eng. Asp. 265 (1–3), 32–39. https://doi.org/10.1016/j.colsurfa.2004.11.051.

Lee, S.Y., Park, S.J., 2014. Carbon dioxide adsorption performance of ultramicroporous carbon derived from poly(vinylidene fluoride). J. Anal. Appl. Pyrol. 106, 147–151. https://doi.org/10.1016/j.jaap.2014.01.012.

Li, J.R., Ma, Y., McCarthy, M.C., Sculley, J., Yu, J., Jeong, H.K., Balbuena, P.B., Zhou, H. C., 2011. Carbon dioxide capture-related gas adsorption and separation in

metalorganic frameworks. Coord. Chem. Rev. 255 (15–16), 1791–1823. https://doi.org/10.1016/j.ccr.2011.02.012.
Li, Z., Wang, K., Song, J., Xu, Q., Kobayashi, N., 2014. Preparation of activated carbons from polycarbonate with chemical activation using response surface methodology. J. Mater. Cycles Waste Manag. 16 (2), 359–366. https://doi.org/10.1007/s10163-013-0196-8.
Li, Y., Xiao, Y., Dong, H., Zheng, M., Liu, Y., 2019a. Polyacrylonitrile-based highly porous carbon materials for exceptional hydrogen storage. Int. J. Hydrog. Energy 44 (41), 23210–23215. https://doi.org/10.1016/j.ijhydene.2019.07.023.
Li, Y., Liang, Y., Hu, H., Dong, H., Zheng, M., Xiao, Y., Liu, Y., 2019b. KNO_3-mediated synthesis of high-surface-area polyacrylonitrile-based carbon material for exceptional supercapacitors. Carbon 152, 120–127. https://doi.org/10.1016/j.carbon.2019.06.001.
Lian, F., Xing, B., Zhu, L., 2011. Comparative study on composition, structure, and adsorption behavior of activated carbons derived from different synthetic waste polymers. J. Colloid Interface Sci. 360 (2), 725–730. https://doi.org/10.1016/j.jcis.2011.04.103.
Linville, J.L., Shen, Y., Ignacio-de Leon, P.A., Schoene, R.P., Urgun-Demirtas, M., 2017. In-situ biogas upgrading during anaerobic digestion of food waste amended with walnut shell biochar at bench scale. Waste Manage. Res. 35 (6), 669–679. https://doi.org/10.1177/0734242X17704716.
Liou, T.H., Wu, S.J., 2009. Characteristics of microporous/mesoporous carbons prepared from rice husk under base- and acid-treated conditions. J. Hazard. Mater. 171 (1–3), 693–703. https://doi.org/10.1016/j.jhazmat.2009.06.056.
Liu, W.J., Jiang, H., Yu, H.Q., 2015. Development of biochar-based functional materials: Toward a sustainable platform carbon material. Chem. Rev. 115 (22), 12251–12285. https://doi.org/10.1021/acs.chemrev.5b00195.
Liu, P., Wang, Y., Zhou, Z., Yuan, H., Zheng, T., Chen, Y., 2020. Effect of carbon structure on hydrogen release derived from different biomass pyrolysis. Fuel 271, 117638. https://doi.org/10.1016/j.fuel.2020.117638.
Liu, X., Yang, F., Li, M., Wang, S., Sun, C., 2022. From polyvinyl chloride waste to activated carbons: the role of occurring additives on porosity development and gas adsorption properties. Sci. Total Environ. 833, 154894 https://doi.org/10.1016/j.scitotenv.2022.154894.
López, G., Artetxe, M., Amutio, M., Bilbao, J., Olazar, M., 2017. Thermochemical routes for the valorization of waste polyolefinic plastics to produce fuels and chemicals. A review. Renew. Sust. Energ. Rev. 73, 346–368. https://doi.org/10.1016/j.rser.2017.01.142.
López, A., de Marco, I., Caballero, B.M., Laresgoiti, M.F., Adrados, A., 2011a. Dechlorination of fuels in pyrolysis of PVC containing plastic wastes. Fuel Process. Technol. 92 (2), 253–260. https://doi.org/10.1016/j.fuproc.2010.05.008.
López, A., de Marco, I., Caballero, B.M., Laresgoiti, M.F., Adrados, A., 2011b. Influence of time and temperature on pyrolysis of plastic wastes in a semi-batch reactor. Chem. Eng. J. 173 (1), 62–71. https://doi.org/10.1016/j.cej.2011.07.037.
López, G., Olazar, M., Aguado, R., Bilbao, J., 2010. Continuous pyrolysis of waste tyres in a conical spouted bed reactor. Fuel 89 (8), 1946–1952. https://doi.org/10.1016/j.fuel.2010.03.029.
Lourenco, M.A.O., Nunes, C., Gomes, J.B.R., Pires, J., Pinto, M.L., Ferreira, P., 2019. Pyrolyzed chitosan-based materials for CO_2/CH_4 separation. Chem. Eng. J. 362, 364–374. https://doi.org/10.1016/j.cej.2018.12.180.
Lozano-Castelló, D., Lillo-Ródenas, M.A., Cazorla-Amorós, D., Linares-Solano, A., 2001. Preparation of activated carbons from Spanish anthracite: I. Activation by KOH. Carbon 39 (5), 741–749. https://doi.org/10.1016/S0008-6223(00)00185-8.
Lozano-Castelló, D., Cazorla-Amorós, D., Linares-Solano, A., 2004. Usefulness of CO_2 adsorption at 273 K for the characterization of porous carbons. Carbon 42 (7), 1233–1242. https://doi.org/10.1016/J.CARBON.2004.01.037.
Ludlow-Palafox, C., Chase, H.A., 2001. Microwave-induced pyrolysis of plastic wastes. Ind. Eng. Chem. Res. 40 (22), 4749–4756. https://doi.org/10.1021/ie010202j.
Machado, N.C.F., de Jesus, L.A.M., Pinto, P.S., de Paula, F.G.F., Alves, M.O., Mendes, K. H.A., Mambrini, R.V., Barrreda, D., Rocha, V., Santamaría, R., Trigueiro, J.P.C., Lavall, R.L., Ortega, P.F.R., 2021. Waste-polystyrene foams-derived magnetic carbon material for adsorption and redox supercapacitor applications. J. Clean. Prod. 313, 127903 https://doi.org/10.1016/j.jclepro.2021.127903.
Maddah, B., Nasouri, K., 2015. Fabrication of high surface area PAN-based activated carbon fibers using response surface methodology. Fiber. Polym. 16 (10), 2141–2147. https://doi.org/10.1007/s12221-015-5514-4.
Martínez-Alonso, A., Jamond, M., Montes-Morán, M.A., Tascón, J.M.D., 1997. Microporous texture of activated carbon fibers prepared from aramid fiber pulp. Microporous Mater. 11 (5–6), 303–311. https://doi.org/10.1016/S0927-6513(97)00050-3.
Martín-Lara, M.A., Piñar, A., Ligero, A., Blázquez, G., Calero, M., 2021. Characterization and use of char produced from pyrolysis of post-consumer mixed plastic waste. Water 13 (9), 1188. https://doi.org/10.3390/w13091188.
Marzec, M., Tryba, B., Kalenczuk, R.J., Morawski, A.W., 1999. Poly(ethylene terephthalate) as a source for activated carbon. Polym. Adv. Technol. 10 (10), 588–595. https://doi.org/10.1002/(SICI)1099-1581(199910).
Méndez-Liñán, L., López-Garzón, F.J., Domingo-García, M., Pérez-Mendoza, M., 2010. Carbon Adsorbents from Polycarbonate Pyrolysis Char Residue: Hydrogen and Methane Storage Capacities. Energy Fuels 24 (6), 3394–3400. https://doi.org/10.1021/ef901525b.
Mestre, A.S., Pires, J., Nogueira, J.M.F., Parra, J.B., Carvalho, A.P., Ania, C.O., 2009. Waste-derived activated carbons for removal of ibuprofen from solution: Role of surface chemistry and pore structure. Bioresour. Technol. 100 (5), 1720–1726. https://doi.org/10.1016/j.biortech.2008.09.039.
Miandad, R., Nizami, A.S., Rehan, M., Barakat, M.A., Khan, M.I., Mustafa, A., Ismail, I.M. I., Murphy, J.D., 2016. Influence of temperature and reaction time on the conversion of polystyrene waste to pyrolysis liquid oil. Waste Manag. 58, 250–259. https://doi.org/10.1016/j.wasman.2016.09.023.
Miskolczi, N., Bartha, L., Deák, G., Jóver, B., Kalló, D., 2004. Thermal and thermo-catalytic degradation of high-density polyethylene waste. J. Anal. Appl. Pyrol. 72 (2), 235–242. https://doi.org/10.1016/j.jaap.2004.07.002.
Moura, P.A.S., Bezerra, D.P., Vilarrasa-Garcia, E., Bastos-Neto, M., Azevedo, D.C.S., 2016. Adsorption equilibria of CO_2 and CH_4 in cation-exchanged zeolites 13X. Adsorption 22 (1), 71–80. https://doi.org/10.1007/s10450-015-9738-9.
Moura, P.A.S., Vilarrasa-Garcia, E., Maia, D.A.S., Bastos-Neto, M., Ania, C.O., Parra, J.B., Azevedo, D.C.S., 2018. Assessing the potential of nanoporous carbon adsorbents from polyethylene terephthalate (PET) to separate CO_2 from flue gas. Adsorption 24 (3), 279–291. https://doi.org/10.1007/s10450-018-9943-4.
Mui, E.L.K., Cheung, W.H., McKay, G., 2010. Tyre char preparation from waste tyre rubber for dye removal from effluents. J. Hazard. Mater. 175 (1–3), 151–158. https://doi.org/10.1016/j.jhazmat.2009.09.142.
Mulu, E., M'Arimi, M.M., Ramkat, R.C., 2021. A review of recent developments in application of low cost natural materials in purification and upgrade of biogas. Renew. Sust. Energ. Rev. 145, 111081 https://doi.org/10.1016/j.rser.2021.111081.
Nakagawa, K., Tamon, H., Suzuki, T., Nagano, S., 2000. Improvement of mesoporosity of activated carbons from PET by novel pre-treatment for steam activation. Adsorpt. Sci. Technol. 456–460. https://doi.org/10.1142/9789812793331_0091.
Nakagawa, K., Mukai, S.R., Suzuki, T., Tamon, H., 2003. Gas adsorption on activated carbons from PET mixtures with a metal salt. Carbon 41 (4), 823–831. https://doi.org/10.1016/S0008-6223(02)00404-9.
Nakagawa, K., Namba, A., Mukai, S.R., Tamon, H., Ariyadejwanich, P., Tanthapanichakoon, W., 2004. Adsorption of phenol and reactive dye from aqueous solution on activated carbons derived from solid wastes. Water Res. 38 (7), 1791–1798. https://doi.org/10.1016/j.watres.2004.01.002.
Nagano, S., Tamon, H., Adzumi, T., Nakagawa, K., Suzuki, T., 2000. Activated carbon from municipal waste. Carbon 38 (6), 915–920. https://doi.org/10.1016/S0008-6223(99)00208-0.
Namane, A., Mekarzia, A., Benrachedi, K., Bensemra, N.B., Hellal, A., 2005. Determination of the adsorption capacity of activated carbon made from coffee grounds by chemical activation with ZnCl2 and H3PO4. J. Hazard. Mater. 119 (1–3), 189–194. https://doi.org/10.1016/j.jhazmat.2004.12.006.
Nsakala, N.Y., Essenhigh, R.H., Walker, P.L., 1978. Characteristics of chars produced from lignites by pyrolysis at 808-degrees-C following rapid heating. Fuel 57, 605–611. https://doi.org/10.1016/0016-2361(78)90189-8.
Onwudili, J.A., Insura, N., Williams, P.T., 2009. Composition of products from the pyrolysis of polyethylene and polystyrene in a closed batch reactor: Effects of temperature and residence time. J. Anal. Appl. Pyrol. 86 (2), 293–303. https://doi.org/10.1016/j.jaap.2009.07.008.
Pallarés, J., González-Cencerrado, A., Arauzo, I., 2018. Production and characterization of activated carbon from barley straw by physical activation with carbon dioxide and steam. Biomass Bioenergy 115, 64–73. https://doi.org/10.1016/j.biombioe.2018.04.015.
Park, H.Y., Lee, C.H., Cho, D.W., Lee, C.H., Park, J.H., 2020. Synthesis of porous carbon derived from poly(vinylidenefluoride) and its adsorption characteristics for CO_2 and CH_4. Microporous and Mesoporous Mat. 299, 110121 https://doi.org/10.1016/j.micromeso.2020.110121.
Parra, J.B., Ania, C.O., Arenillas, A., Rubiera, F., Pis, J.J., Palacios, J.M., 2006. Structural Changes in Polyethylene Terephthalate (PET) Waste Materials Caused by Pyrolysis and CO_2 Activation. Adsorpt. Sci. Technol. 24 (5), 439–450. https://doi.org/10.1260/026361706779849735.
Peng, W.M., Wu, Q.Y., Tu, P.G., 2000. Effects of temperature and holding time on production of renewable fuels from pyrolysis of *Chlorella protothecoides*. J. Appl. Phycol. 12 (2), 147–152. https://doi.org/10.1023/a:1008115025002.
Podkościelny, P., László, K., 2007. Heterogeneity of activated carbons in adsorption of aniline from aqueous solutions. Appl. Surf. Sci. Volume 253 (21), 8762–8771. https://doi.org/10.1016/j.apsusc.2007.04.057.
Przepiórski, J., Czyżewski, A., Pietrzak, R., Morawski, A.W., 2013. MgO/CaO-Loaded Activated Carbon for Carbon Dioxide Capture: Practical Aspects of Use. Ind. Eng. Chem. Res. 52 (20), 6669–6677. https://doi.org/10.1021/ie302848r.
Quesada, L., Pérez, A., Godoy, V., Peula, F.J., Calero, M., Blázquez, G., 2019. Optimization of the pyrolysis process of a plastic waste to obtain a liquid fuel using different mathematical models. Energy Conv. Manag. 188, 19–26. https://doi.org/10.1016/j.enconman.2019.03.054.
Qiao, W.M., Yoon, S.H., Korai, Y., Mochida, I., Inoue, S., Sakurai, T., Shimohara, T., 2004. Preparation of activated carbon fibers from polyvinyl chloride. Carbon 42 (7), 1327–1331. https://doi.org/10.1016/j.carbon.2004.01.035.
Qureshi, M.S., Oasmaa, A., Pihkola, H., Deviatkin, I., Tenhunen, A., Mannila, J., Minkkinen, H., Pohjakallio, M., Laine-Ylijoki, J., 2020. Pyrolysis of plastic waste: Opportunities and challenges. J. Anal. Appl. Pyrol. 152, 104804 https://doi.org/10.1016/j.jaap.2020.104804.
Rai, P., Singh, K.P., 2018. Valorization of Poly (ethylene) terephthalate (PET) wastes into magnetic carbon for adsorption of antibiotic from water: characterization and application. J. Environ. Manag. 207, 249–261. https://doi.org/10.1016/j.jenvman.2017.11.047.
Rehman, A., Park, S.J., 2018a. Comparative study of activation methods to design nitrogen-doped ultra-microporous carbons as efficient contenders for CO_2 capture. Chem. Eng. J. 352, 539–548. https://doi.org/10.1016/j.cej.2018.07.046.
Rehman, A., Park, S.J., 2018b. Microporous carbons derived from melamine and isophthalaldehyde: one-pot condensation and activation in a molten salt medium for e cient gas adsorption. Sci. Rep. 8 (1), 6092. https://doi.org/10.1038/s41598-018-24308-z.

Ren, X., Zhang, C., Kou, L., Wang, R., Wang, Y., Li, R., 2022. Hierarchical porous polystyrene-based activated carbon spheres for CO_2 capture. Environ. Sci. Pollut. Res. Int. 29 (9), 13098–13113. https://doi.org/10.1007/s11356-021-16561-z.
Rodríguez-Reinoso, F., Molina-Sabio, M., 1992. Activated carbons from lignocellulosic materials by chemical and/or physical activation: an overview. Carbon 30 (7), 1111–1118. https://doi.org/10.1016/0008-6223(92)90143-K.
Rodríguez-Reinoso, F., Molina-Sabio, M., González, M.T., 1995. The use of steam and CO_2 as activating agents in the preparation of activated carbons. Carbon 33 (1), 15–23. https://doi.org/10.1016/0008-6223(94)00100-E.
Rosi, L., Bartoli, M., Frediani, M., 2018. Microwave assisted pyrolysis of halogenated plastics recovered from waste computers. Waste Manag. 73, 511–522. https://doi.org/10.1016/j.wasman.2017.04.037.
Ryu, Z., Zheng, J., Wang, M., Zhang, B., 2000. Nitrogen Adsorption Studies of PAN-Based Activated Carbon Fibers Prepared by Different Activation Methods. J. Colloid Interf. Sci. 230 (2), 312–319. https://doi.org/10.1006/jcis.2000.7078.
Saad, M.J., Chia, C.H., Zakaria, S., Sajab, M.S., Misran, S., Abdul Rahman, M.H., Chin, S. X., 2019. Physical and chemical properties of the rice straw activated carbon produced from carbonization and KOH activation processes. Sains Malays. 48 (2), 385–391. https://doi.org/10.17576/jsm-2019-4802-16.
Saptoadi, H., Rohmat, T.A., Sutoyo, 2016. Combustion of char from plastic wastes pyrolysis. AIP Conf. Proc. 1737, 30006. https://doi.org/10.1063/1.4949286.
Serrano, D.P., Aguado, J., Escola, J.M., Garagorri, E., 2001. Conversion of low density polyethylene into petrochemical feedstocks using a continuous screw kiln reactor. J. Anal. Appl. Pyrol. 58–59, 789–801. https://doi.org/10.1016/S0165-2370(00)00153-4.
Seo, D.-J., Gou, Z., Fujita, H., Fujii, T., Sakoda, A., 2016. Simple fabrication of molecular sieving carbon for biogas upgrading via a temperature controlled carbonization of *Phyllostachys pubescens*. Renew. Energ. 86, 693–702. https://doi.org/10.1016/j.renene.2015.09.006.
Sevilla, M., Fuertes, A.B., 2011. Sustainable porous carbons with a superior performance for CO_2 capture. Energ. Environ. Sci. 4 (5), 1765. https://doi.org/10.1039/C0EE00784F.
Sevilla, M., Mokaya, R., 2014. Energy storage applications of activated carbons: supercapacitors and hydrogen storage. Energ. Environ. Sci. 7 (4), 1250–1280. https://doi.org/10.1039/C3EE43525C.
Shafeeyan, M.S., Daud, W.M.A.W., Houshmand, A., Shamiri, A., 2010. A review on surface modification of activated carbon for carbon dioxide adsorption. J. Anal. Appl. Pyrol. 89, 143–151. https://doi.org/10.1016/j.jaap.2010.07.006.
Sharuddin, S.D.A., Abnisa, F., Daud, W.M.A.W., Aroua, M.K., 2016. A review on pyrolysis of plastic wastes. Energ. Conver. Manage. 115, 308–326. https://doi.org/10.1016/j.enconman.2016.02.037.
Shen, W., Zhang, S., He, Y., Li, J., Fan, W., 2011. Hierarchical porous polyacrylonitrile-based activated carbon fibers for CO_2 capture. J. Mater. Chem. 21 (36), 14036. https://doi.org/10.1039/C1JM12585K.
Scott, D.S., Czernik, S.R., Piskorz, J., Radlein, D.S.A.G., 1990. Fast pyrolysis of plastic waste. Energy Fuels 4, 407–411. https://doi.org/10.1021/ef00022a013.
Sing, K.S.W., 1995. In: Patrick, J.W., Arnold, Edward (Eds.), Porosity in carbons: characterization and applications 2, 49.
Singh, J., Laurenti, R., Sinha, R., Frostell, B., 2014. Progress and challenges to the global waste management system. Waste Manag. Res. 32 (9), 800–812. https://doi.org/10.1177/0734242X14537868.
Singh, R.K., Ruj, B., 2016. Time and temperature depended fuel gas generation from pyrolysis of real world municipal plastic waste. Fuel 174, 164–171. https://doi.org/10.1016/j.fuel.2016.01.049.
Singh, R.K., Ruj, B., Sadhukhan, A.K., Gupta, P., 2019a. Impact of fast and slow pyrolysis on the degradation of mixed plastic waste: product yield analysis and their characterization. J. Energy Inst. 92 (6), 1647–1657. https://doi.org/10.1016/j.joei.2019.01.009.
Singh, J., Basu, S., Bhunia, H., 2019b. Dynamic CO_2 adsorption on activated carbon adsorbents synthesized from polyacrylonitrile (PAN): Kinetic and isotherm studies. Microporous Mesoporous Mat. 280, 357–366. https://doi.org/10.1016/j.micromeso.2019.02.031.
Singh, J., Bhunia, H., Basu, S., 2019c. Adsorption of CO_2 on KOH activated carbon adsorbents: Effect of different mass ratios. J. Environ. Manage. 250, 109457 https://doi.org/10.1016/j.jenvman.2019.109457.
Singh, J., Basu, S., Bhunia, H., 2019d. CO_2 capture by modified porous carbon adsorbents: Effect of various activating agents. J. Taiwan Inst. Chem. Eng. 102, 438–447. https://doi.org/10.1016/j.jtice.2019.06.011.
Solis, M., Silveira, S., 2020. Technologies for chemical recycling of household plastics - a technical review and TRL assessment. Waste Manag. 105, 128–138. https://doi.org/10.1016/j.wasman.2020.01.038.
Song, C., Zhang, B., Hao, L., Min, J., Liu, N., Niu, R., Gong, J., Tang, T., 2020. Converting poly(ethylene terephthalate) waste into N-doped porous carbon as CO_2 adsorbent and solar steam generator. Green Energy Environ. 7 (3), 411–422. https://doi.org/10.1016/j.gee.2020.10.002.
Sureshkumar, A., Susmita, M., 2018. Optimization of preparation conditions for activated carbons from polyethylene terephthalate using response surface methodology. Braz. J. Chem. Eng. 35 (3), 1105–1116. https://doi.org/10.1590/0104-6632.20180353s20160724.
Surra, E., Ribeiro, R., Santos, T., Bernardo, M., Mota, J.P.B., Lapa, N., Esteves, I., 2022. Evaluation of activated carbons produced from Maize Cob Waste for adsorption-based CO_2 separation and biogas upgrading. J. Environ. Chem. Eng. (10),, 107065. https://doi.org/10.1016/j.jece.2021.107065.
Sun, Y., Zhao, J., Wang, J., Tang, N., Zhao, R., Zhang, D., Guan, T., Li, K., 2017. Sulfur-Doped millimeter-sized microporous activated carbon spheres derived from sulfonated poly (styrene-divinylbenzene) for CO_2 capture. J. Phys. Chem. C 121 (18), 10000–10009. https://doi.org/10.1021/acs.jpcc.7b02195.
Sych, N.V., Kartel, N.T., Tsyba, N.N., Strelko, V.V., 2006. Effect of combined activation on the preparation of high porous active carbons from granulated post-consumer polyethyleneterephthalate. Appl. Surf. Sci. 252 (23), 8062–8066. https://doi.org/10.1016/j.apsusc.2005.10.009.
Syamsiro, M., Saptoadi, H., Norsujianto, T., Noviasri, P., 2014. Fuel Oil Production from Municipal Plastic Wastes in Sequential Pyrolysis and Catalytic Reforming Reactors. Energy Procedia 47, 180–188. https://doi.org/10.1016/j.egypro.2014.01.212.
Tsuchiya, Y., Yamaya, Y., Amano, Y., Machida, M., 2021. Effect of two types of adsorption sites of activated carbon fibers on nitrate ion adsorption. J. Environ. Manage. 289, 112484 https://doi.org/10.1016/j.jenvman.2021.112484.
Uddin, M.A., Koizumi, K., Murata, K., Sakata, Y., 1997. Thermal and catalytic degradation of structurally different types of polyethylene into fuel oil. Polym. Degrad. Stabil. 56 (1), 37–44. https://doi.org/10.1016/S0141-3910(96)00191-7.
UNEP, 2021a - From Pollution to Solution: A Global Assessment of Marine Litter and Plastic Pollution. https://www.unep.org/interactive/pollution-to-solution/ (accessed 03 May 2022).
UNEP, 2021b Drowning in Plastics – Marine Litter and Plastic Waste Vital Graphics. https://www.unep.org/resources/report/drowning-plastics-marine-litter-and-plastic-waste-vital-graphics (accessed 03 May 2022).
Vilella, P.C., Lira, J.A., Azevedo, D.C.S., Bastos-Neto, M., Stefanutti, R., 2017. Preparation of biomass-based activated carbons and their evaluation for biogas upgrading purposes. Ind. Crop Prod. 109, 134–140. https://doi.org/10.1016/j.indcrop.2017.08.017.
Vivo-Vilches, J.F., Pérez-Cadenas, A.F., Maldonado-Hódar, F.J., Carrasco-Marín, F., Faria, R.P.V., Ribeiro, A.M., Ferreira, A.F.P., Rodrigues, A.E., 2017. Biogas upgrading by selective adsorption onto CO_2 activated carbon from wood pellets. J. Environ. Chem. Eng. 5 (2), 1386–1393. https://doi.org/10.1016/j.jece.2017.02.015.
Wallis, M.D., Sarathy, S., Bhatia, S.K., Massarotto, P., Kosior, E., Mercier, A., 2008. Catalytic degradation of high-density polyethylene in a reactive extruder. Ind. Eng. Chem. Res. 47 (15), 5175–5181. https://doi.org/10.1021/ie0714450.
Wang, Q., Liang, X.Y., Qiao, W.M., Liu, C.J., Liu, X.J., Zhan, L.A., Ling, L.C., 2009. Preparation of polystyrene-based activated carbon spheres with high surface area and their adsorption to dibenzothiophene. Fuel Process. Technol. 90 (3), 381–387. https://doi.org/10.1016/j.fuproc.2008.10.008.
Wang, J., Kaskel, S., 2012. KOH activation of carbon-based materials for energy storage. J. Mater. Chem. 22 (45), 23710–23725. https://doi.org/10.1039/C2JM34066F.
Wang, B., Zhu, C., Zhang, Z., Zhang, W., Chen, X., Sun, N., Wei, W., Sun, Y., Ji, H., 2016. Facile, low-cost, and sustainable preparation of hierarchical porous carbons from ion exchange resin: an improved potassium activation strategy. Fuel 179, 274–280. https://doi.org/10.1016/j.fuel.2016.03.088.
Wang, L., Wang, Y., Ma, F., Tankpa, V., Bai, S., Guo, X., Wang, X., 2019. Mechanisms and reutilization of modified biochar used for removal of heavy metals from wastewater: a review. Sci. Total Environ. 668, 1298–1309. https://doi.org/10.1016/j.scitotenv.2019.03.011.
Wang, J., Yuan, X., Deng, S., Zeng, X., Yu, Z., Li, S., Li, K., 2020a. Waste polyethylene terephthalate (PET) plastics-derived activated carbon for CO_2 capture: a route to a closed carbon loop. Green Chem. 22 (20), 6836–6845. https://doi.org/10.1039/D0GC01613F.
Wang, J., Wang, F., Duan, H., Li, Y., Xu, J., Huang, Y., Liu, B., Zhang, T., 2020b. Polyvinyl chloride-derived carbon spheres for CO_2 adsorption. Chem. Sus. Chem 13 (23), 6426–6432. https://doi.org/10.1002/cssc.202002230.
Wang, H., Xu, J., Liu, X., Sheng, L., 2021. Preparation of straw activated carbon and its application in wastewater treatment: A review. J. Clean. Prod. 283, 124671 https://doi.org/10.1016/j.jclepro.2020.124671.
Williams, P.T., Slaney, E., 2007. Analysis of products from the pyrolysis and liquefaction of single plastics and waste plastic mixtures. Resour. Conserv. Recycl. 51 (4), 754–769. https://doi.org/10.1016/j.resconrec.2006.12.002.
Williams, E.A., Williams, P.T., 1997a. Analysis of products derived from the fast pyrolysis of plastic waste. J. Anal. Appl. Pyrol. 40–41, 347–363. https://doi.org/10.1016/S0165-2370(97)00048-X.
Williams, E.A., Williams, P.T., 1997b. The pyrolysis of individual plastics and a plastic mixture in a fixed bed reactor. J. Chem. Technol. Biotechnol. 70 (1), 9–20. https://doi.org/10.1002/(SICI)1097-4660(199709)70:1<9::AID-JCTB700>3.0.CO;2-E.
Xian, S., Wu, Y., Wu, J., Wang, X., Xiao, J., 2015. Enhanced dynamic CO_2 adsorption capacity and CO_2/CH_4 Selectivity on polyethylenimine-impregnated UiO-66. Ind. Eng. Chem. Res. 54 (44), 11151–11158. https://doi.org/10.1021/acs.iecr.5b03517.
Yahya, M.A., Al-Qodah, Z., Ngah, C.Z., 2015. Agricultural bio-waste materials as potential sustainable precursors used for activated carbon production: a review. Renew. Sustain. Energy Rev. 46, 218–235. https://doi.org/10.1016/j.rser.2015.02.051.
Yuan, X., Lee, J.G., Yun, H., Deng, S., Kim, Y.J., Lee, J.E., Kwak, S.K., Lee, K.B., 2020a. Solving two environmental issues simultaneously: Waste polyethylene terephthalate plastic bottle-derived microporous carbons for capturing CO_2. Chem. Eng. J. 397, 125350 https://doi.org/10.1016/j.cej.2020.125350.
Yuan, X., Li, S., Jeon, S., Deng, S., Zhao, L., Lee, K.B., 2020b. Valorization of waste polyethylene terephthalate plastic into N-doped microporous carbon for CO_2 capture through a one-pot synthesis. J. Hazard. Mater. 399, 123010 https://doi.org/10.1016/j.jhazmat.2020.123010.
Yuliusman, N., Sanal, A., Bernama, A., Haris, F., Ramadhan, I.T., 2017. Preparation of activated carbon from waste plastics polyethylene terephthalate as adsorbent in natural gas storage. IOP Conf. Series. Mater. Sci. Eng. 176, 012055 https://doi.org/10.1088/1757-899X/176/1/012055.

Zhang, X.Q., Li, W.C., Lu, A.H., 2015. Designed porous carbon materials for efficient CO_2 adsorption and separation. New Carbon Mater. 30 (6), 481–501. https://doi.org/10.1016/S1872-5805(15)60203-7.

Zhang, Y., Cui, Y., Liu, S., Fan, L., Zhou, N., Peng, P., Wang, Y., Guo, F., Min, M., Cheng, Y., Liu, Y., Lei, H., Chen, P., Li, B., Ruan, R., 2020. Fast microwave-assisted pyrolysis of wastes for biofuels production – A review. Bioresour. Technol. 297, 122480 https://doi.org/10.1016/j.biortech.2019.122480.

Zhang, H., Zhou, X., Shao, L., Lü, F., He, P., 2021. Upcycling of PET waste into methane-rich gas and hierarchical porous carbon for high-performance supercapacitor by autogenic pressure pyrolysis and activation. Sci. Total Environ. 772, 145309 https://doi.org/10.1016/j.scitotenv.2021.145309.

Zheng, J., Suh, S., 2019. Strategies to reduce the global carbon footprint of plastics. Nat. Clim. Chang. 9 (5), 374–378. https://doi.org/10.1038/s41558-019-0459-z.

Zhong, Z.Y., Yang, Q., Li, X.M., Luo, K., Liu, Y., Zeng, G.M., 2012. Preparation of peanut hull- based activated carbon by microwave-induced phosphoric acid activation and its application in Remazol Brilliant Blue R adsorption. Ind. Crop. Prod. 37 (1), 178–185. https://doi.org/10.1016/j.indcrop.2011.12.015.

Zhu, X., Gao, Y., Yue, Q., Kan, Y., Kong, W., Gao, B., 2017. Preparation of green alga-based activated carbon with lower impregnation ratio and less activation time by potassium tartrate for adsorption of chloramphenicol. Ecotox. Environ. Safe. 145, 289–294. https://doi.org/10.1016/j.ecoenv.2017.07.053.